Clinical utility of NGS diagnosis and disease stratification in a multi-ethnic primary ciliary dyskinesia cohort

Mahmoud R. Fassad [1,2], Mitali P. Patel [1], Amelia Shoemark [3,4], Thomas Cullup [5], Jane Hayward [5], Mellisa Dixon [3], Andrew V Rogers [6], Sarah Ollosson [3], Claire Jackson [7,8], Patricia Goggin [7,8], Robert A. Hirst [9], Andrew Rutman [9], James Thompson [7,8], Lucy Jenkins [5], Paul Aurora [10,11], Eduardo Moya [12], Philip Chetcuti [13], Christopher O'Callaghan [9,11], Deborah Morris-Rosendahl [14], Christopher M. Watson [15], Robert Wilson [6], Siobhan Carr [3], Woolf Walker [7,8], Andreia Pinto [16], Susana Lopes [17], Heba Morsy [2], Walaa Shoman [18], Luísa Pereira [19], Carolina Constant [19], Michael R Loebinger [6], Eddie MK Chung [20], Priti Kenia [21], Nisreen Rumman [22], Nader Fasseeh [18], Jane S. Lucas [7,8], Claire Hogg [3], Hannah M. Mitchison [1]

[1]Genetics and Genomic Medicine Programme, University College London, UCL Great Ormond Street Institute of Child Health, London WC1N 1EH, UK
[2]Department of Human Genetics, Medical Research Institute, Alexandria University, 165 El-Horreya Avenue, El- Hadra 21561, Alexandria, Egypt
[3]PCD Diagnostic Team and Department of Pediatric Respiratory Medicine, Royal Brompton and Harefield NHS Trust, London SW3 6NP, UK
[4]Division of Molecular and Clinical Medicine, University of Dundee, Ninewells Hospital and Medical School, Dundee DD1 9SY, UK
[5]Regional Molecular Genetics Laboratory, Great Ormond Street Hospital for Children NHS Foundation Trust, Queen Square, London WC1N 3BH, UK
[6]Host Defence Unit, Royal Brompton and Harefield NHS Trust, Sydney Street, London SW3 6NP, UK
[7]Primary Ciliary Dyskinesia Centre, University Hospital Southampton NHS Foundation Trust and Clinical and Experimental Sciences Academic Unit, University of Southampton Faculty of Medicine, Southampton SO17 1BJ, UK
[8]NIHR Southampton Biomedical Research Centre, University of Southampton and University Hospital Southampton NHS Foundation Trust, Southampton SO16 6YD, UK
[9]Centre for PCD Diagnosis and Research, Department of Infection, Immunity and Inflammation, RKCSB, University of Leicester, Leicester LE2 7LX, UK
[10]Department of Paediatric Respiratory Medicine, Great Ormond Street Hospital for Children, London WC1N 3JH, UK.
[11]Department of Respiratory, Critical Care and Anaesthesia Unit, University College London (UCL) Great Ormond Street Institute of Child Health, Guilford Street, London WC1N 1EH, UK.
[12]Division of Services for Women and Children, Women's and Newborn Unit, Primary Ciliary Dyskinesia Centre, Bradford Royal Infirmary, Bradford, UK.
[13]Department of Respiratory Paediatrics, Leeds General Infirmary, Leeds Teaching Hospitals NHS Trust, Leeds LS1 3EX, UK.
[14]Clinical Genetics and Genomics Laboratory, Royal Brompton and Harefield NHS Foundation Trust, London SW3 6NP, UK
[15]Leeds Genetics Laboratory, Leeds Teaching Hospitals NHS Trust, Leeds, LS9 7TF, UK
[16]Laboratório de Histologia e Patologia Comparada, Instituto de Medicina Molecular, Centro Académico de Medicina de Lisboa, Lisboa, Portugal
[17]CEDOC, Faculdade de Ciências Médicas, Universidade Nova de Lisboa, 1169-056 Lisboa, Portugal

[18]Department of Pediatrics, Faculty of Medicine, Alexandria University Children's Hospital, Egypt

[19]Paediatric Pulmonology Unit, Department of Paediatrics, Hospital de Santa Maria, Centro Hospitalar Lisboa Norte, Centro Académico de Medicina de Lisboa, Lisbon, Portugal.

[20]Population, Policy and Practice Programme, University College London, UCL Great Ormond Street Institute of Child Health, London WC1N 1EH, UK

[21]Department of Respiratory Paediatrics, Birmingham Women's and Children's Hospital NHS Foundation Trust, Steelhouse Lane, Birmingham B4 6NH, UK

[22]Pediatrics Department, Makassed Hospital, East Jerusalem, Palestine

Corresponding author:
Dr Hannah Mitchison
Genetics and Genomic Medicine, UCL Great Ormond Street Institute of Child Health,
30 Guilford Street, London WC1N 1EH
Fax. +44 (0)20 7404 6191; Tel. +44 (0)20 7905 2866; Email. h.mitchison@ucl.ac.uk

Word count: 3,570.

Key words: primary ciliary dyskinesia, mutation spectrum, cilia, bronchiectasis, population

ABSTRACT

Background: Primary ciliary dyskinesia (PCD), a genetically heterogeneous condition enriched in some consanguineous populations, results from recessive mutations affecting cilia biogenesis and motility. Currently, diagnosis requires multiple expert tests.

Methods: The diagnostic utility of multi-gene panel next-generation sequencing (NGS) was evaluated in 161 unrelated families from multiple population ancestries.

Results: Most (82%) families had affected individuals with biallelic or hemizygous (75%) or single (7%) pathogenic causal alleles in known PCD genes. Loss-of-function alleles dominate (73% frameshift, stop-gain, splice site), most (58%) being homozygous, even in non-consanguineous families. Although 57% (88) of the total 155 diagnostic disease variants were novel, recurrent mutations and mutated genes were detected. These differed markedly between White European (52% of families carry *DNAH5* or *DNAH11* mutations), Arab (42% of families carry *CCDC39* or *CCDC40* mutations) and South Asian (single *LRRC6* or *CCDC103* mutations carried in 36% of families) patients, revealing a striking genetic stratification according to population of origin in PCD. Genetics facilitated successful diagnosis of 81% of families with normal or inconclusive ultrastructure and 67% missing prior ultrastructure results.

Conclusions: This study shows the added value of high-throughput targeted NGS in expediting PCD diagnosis. Therefore, there is potential significant patient benefit in wider and/or earlier implementation of genetic screening.

INTRODUCTION

Primary ciliary dyskinesia (PCD) is a rare genetic disease caused by cilia dysmotility that is associated with a range of defects of motile cilia structure and biogenesis. PCD is typically an autosomal or X-linked recessive disorder, caused by mutations in >40 different genes encoding structural ciliary proteins, cilia assembly and transport factors and proteins implicated in multi-ciliogenesis[1, 2]. Children and adults affected by PCD consequently manifest with progressive respiratory disease characterized by bronchiectasis and impaired lung function. Symptoms often present in early life with neonatal respiratory distress syndrome and persist with chronic wet cough, rhinitis, sinusitis, otitis media and hearing defects[3]. Defective cilia of the brain ependyma, fallopian tubes, and developing embryo can explain other disease features. Half of patients have laterality defects arising from embryonic nodal cilia dysfunction and a significant proportion of males are subfertile with defective sperm flagella. Affected individuals, in particular those with reduced cilia numbers, can also manifest with hydrocephalus, while *RPGR* and *OFD1* mutations can respectively cause rare retinal dystrophy and oral-facial-digital syndrome PCD subtypes[1, 2, 4, 5].

The prevalence of PCD is around 1:15,000 worldwide. PCD occurs much more frequently in highly consanguineous communities such as the UK South Asian population, in whom disease prevalence is as high as 1:2,265[3]. Generally, PCD symptoms are variable and diagnosis is frequently delayed or missed[6]. Early diagnosis has potential to improve morbidity since lung damage can be delayed by specialist care[3, 7]. PCD diagnostic testing requires access to a combination of investigations including measurement for low nasal nitric oxide levels, high

speed video microscopy for ciliary beating defects, ciliary ultrastructure defects analysed by transmission electron microscopy (TEM), immunofluorescence staining for abnormal motile cilia proteins and, increasingly, genetic analysis[7, 8].

PCD genetic diagnosis requires the identification of biallelic autosomal or hemizygous X-linked mutations[7, 8]. Mutations in known PCD genes are found in 60-70% of tested PCD patients[1, 3]. With additional genes still to be identified, the sensitivity of genetic testing as a 'gold standard' diagnostic test is reduced. However, with progressive identification of the whole 'morbid genome' causing PCD and ongoing reductions in DNA sequencing costs, genetics can increasingly be considered as a first line test in the diagnostic pathway. Gene panels can currently be more effective for target sequence coverage and reduced time and costs, than whole exome or genome sequencing[9].

Here, we present a targeted next generation sequencing (NGS) gene panel approach for characterization of a multi-ancestry cohort of PCD patients. Our aim was to investigate the utility of this approach for PCD, a clinically and genetically heterogeneous condition, where current diagnosis requires multiple expert tests[8].

MATERIALS AND METHODS

Subjects

161 unrelated families confirming self-reported ancestry and consanguinity at time of recruitment were ascertained from UK national PCD diagnostic and management services (London Royal Brompton Hospital, University Hospital Southampton, Leeds General Infirmary, Bradford Royal Infirmary, Birmingham Children's Hospital and Leicester Royal Infirmary) and collaborating clinical centres in Portugal (Hospital de Santa Maria, Centro Hospitalar Lisboa Norte, Lisbon), Palestine (Makassed Hospital, East Jerusalem) and Egypt (Alexandria University Children's Hospital, Alexandria). Recruitment took place between 01/2015-02/2017 with informed, age-appropriate consent as approved by the London-Bloomsbury Research Ethics Committee (08/H0713/82) and committees of collaborating institutions. The diagnosis of PCD followed the European Respiratory Society (ERS) guidelines[8], using various methods according to the clinical centre, including clinical presentation and the results of formal PCD diagnostic tests (nasal NO level, cilia ultrastructure analysis by transmission electron microscopy, cilia beat pattern and frequency by high speed video microscopy and immunostaining against specific ciliary proteins). Study inclusion criteria was based upon a clinical suspicion of PCD and/or available cilia ultrastructural TEM analysis. TEM data was not available in a total of 27 families, who were included to the study based upon other clinical criteria suggesting PCD.

Targeted next generation sequencing (NGS)

Genomic DNA extracted from whole blood samples or saliva was screened for mutations using targeted NGS gene panels containing all the known PCD (**online supplementary table S1**) and isolated heterotaxy genes, plus one of two iterations of a larger set of cilia motility associated candidate genes. These were collated after extensive literature searches for candidates with cilia involvement confirmed or likely and from data from previous human genetics and PCD model organisms studies. Panel probe design used the Agilent SureDesign tool (Agilent Technologies, Santa Clara, CA, USA) to capture all coding regions and 25 bp at the exon-intron boundaries (**online supplementary tables S1 and S2**). Capture probes were enriched in regions with potential low coverage. Library preparation used the SureSelectQXT NGS target enrichment kit (Agilent Technologies, Santa Clara, CA, USA) was used for library preparation following the manufacturer's protocol. Paired end sequencing (2 x 150bp) was performed using the NextSeq 500/550 High Output v2 kit and NextSeq sequencing platform (Illumina, Inc., CA, USA). Multiplexing of 48 samples was done on the same flow cell per sequencing run. Sequencing data were processed using an in-house bioinformatics pipeline at North East Thames Regional Genetics Service[10]. Variants were filtered for significance to produce variant lists of interest in each patient that conform to the expected minor allele frequency for PCD (<1%) and an autosomal or X-linked recessive inheritance pattern. Variants were prioritized based on their minor allele frequency in the ExAc database[11], 1,542 individuals in the Born-in-Bradford (BinB) cohort of UK South Asians[12] and the al mena database of genetic variants in Middle East and North African individuals[13]. Potential pathogenicity was assessed using several softwares including Human Splicing Finder, SIFT, Polyphen-2, Mutation Taster and Combined Annotation Dependent Depletion (CADD) score. Variant

7

pathogenicity scoring was done according to the guidelines of the American College of Medical Genetics and Genomics (**online supplementary figure S1**)[14], using a well-established classification (or tiering) system of predicted (i) pathogenic, (ii) likely pathogenic, (iii) uncertain significance, (iv) likely benign, or (v) benign variants. Details of all variants and gene transcript numbers are contained in **online supplementary table S3**. For all affected individuals, a search for large insertion/deletion mutations and copy number variants (using ExomeDepth software) was separately performed[15].

Sanger Sequencing

All prioritized variants were confirmed in the proband and segregated within the available family members using Sanger sequencing. Sequencing data was viewed using SnapGene (GSL Biotech LLC, Chicago, USA) or Sequencher software (Gene Codes Corporation, Ann Arbor, MI, USA).

RESULTS

Targeted NGS yields high diagnostic output in a multi-ancestry cohort of PCD patients

The probands from 161 unrelated families were screened using targeted NGS multi-gene panel analysis, followed by Sanger sequencing-based segregation analysis to confirm all identified genetic variants of interest and determine their familial inheritance pattern. All families had affected individuals with a suggestive clinical phenotype, in addition to either (1) a ciliary

ultrastructural defect confirmed (97 families); or (2) inconclusive TEM results where PCD was still highly suggestive (37 families); or (3) no diagnostic TEM analysis yet performed but PCD still clinically highly suspected (27 families). Their details are summarized in **table 1.** The PCD-consistent features of the total 27 families with probands lacking TEM data are summarized in **online supplementary table S4**. The ancestry and consanguinity of all the families are summarized in **online supplementary table S5**, showing that 46% (74) were European, 22% (35) South-Asian, 18% (29) Arab and the rest had other ancestries. Consanguinity was reported in 29% of 161, with highest levels in the Arab (25; 86%) and South-Asian (12; 34%) families.

TEM ultrastructural phenotype Total no. families (% of 134 with TEM defects defined)	Mutant known PCD gene or novel candidate	No. families
Normal TEM and inconclusive TEM analysis (No apparent defect, or few observed defects insufficient to make a diagnosis) 37 families (28%)	*DNAH11*✝	15
	HYDIN ✝	6
	DNAH5	3
	CCDC103 ✝	2
	RSPH1	1
	OFD1	1
	DNAI2	1
	ZMYND10	1
	Novel candidate gene	4
	Unsolved	3
Outer dynein arm loss 31 families (23%)	*DNAH5*	17
	DNAI1	3
	ARMC4	2
	DNAI2	1
	CCDC151	1
	SPAG1	1
	PIH1D3	1
	Unsolved	5
Combined inner and outer dynein arm loss 30 families (22%)	*LRRC6*	5
	DNAAF3	5
	CCDC103	3
	DNAH5	3
	ZMYND10	2
	DYX1C1	1
	DNAAF1	1
	HEATR2	1
	DNAI1	1
	Novel candidate gene	4*
	Unsolved	4
Microtubular disorganization ± inner dynein arm loss 16 families (12%)	*CCDC40*	7
	CCDC39	5
	CCDC65	1
	RSPH9	1
	RSPH1	1
	Unsolved	1
Central microtubular pair defect 8 families (6%)	*RSPH4A*	4
	RSPH1	2
	RSPH9	1
	Unsolved	1
Inner dynein arm loss 5 families (4%)	*CCDC103*	2
	CCDC164	1
	CCDC40	1
	Novel candidate gene	1**
Lack of cilia cross sections 7 families (5%)	*CCNO*	2
	MCIDAS	2
	DYX1C1	1
	RPGR	1
	Novel candidate gene	1
No TEM analysis 27 families	*CCDC40*	5
	DNAH5	4
	CCDC39	3
	LRRC6	2
	CCDC114	1
	RSPH9	1
	DNAH11	1
	ZMYND10	1
	Novel candidate gene	2
	Unsolved	7

Table 1. Genetic stratification of 161 unrelated PCD families, according to transmission electron microscopy findings. Mutations in genes regarded during the study as candidates but since published as PCD genes were found in *2 families with *CFAP300* and 1 family with *DNAH9* variants; **1 family with *DNAH9* variants [16, 17].✝*DNAH11*, *HYDIN* and often *CCDC103* mutations are associated with normal TEM, whilst the other genes in this group are associated with visible TEM defects [18-20].

We identified causal variants in known PCD genes in 128 of the 161 PCD families, comprising 82% of the cohort (**figure 1A and online supplementary table S3**). Biallelic autosomal or hemizygous X-linked variants were identified in 116 families in known PCD genes and in a further 4 families in genes considered during the study to be candidate genes, comprising two families with *CFAP300* variants[16] and two with *DNAH9* variants[17]. Since these genes have been recently verified as PCD-causing, this means that a total of 120 out of 161 families (75%) were diagnosed. In 12 families (7%), only one mutant allele (single heterozygous) was found in a known autosomal PCD gene, which is considered an incomplete genetic diagnosis, however we include the variant data for all 12 families, since seven are protein truncation variants and 5 are already reported in previous studies on PCD patients; also, all these 'single hit' variant carrying patients had cilia ultrastructural defects consistent with the implicated mutant gene (**figure 1A and online supplementary table S3**).

For 13 families (8%), biallelic variants in candidate genes for PCD (*CFAP300, DNAH9* included at the time) were identified and further functional characterization of these genes and their roles in causing PCD are ongoing. Finally, 20 families (12%), had no putative significant sequence variants, 11 of these having cilia ultrastructural defects identified by TEM and 3 with low nasal nitric oxide and abnormal cilia beat frequency but inconclusive TEM (**online supplementary figure S2**), the other 6 having a strong clinical suspicion of PCD (situs inversus and recurrent respiratory problems) without prior investigations.

Significant, population-based genetic stratification underlies PCD

Prioritized variants for the 128 diagnosed families were identified within different functional categories of known PCD genes (**figure 1B**). The most prevalent, identified in 38% of families, affected genes encoding outer dynein arm (ODA) components (*DNAH5, DNAH11, DNAI1, DNAI2*). The second collectively most common affected genes encoding dynein assembly factors (*LRRC6, DNAAF3, ZMYND10, DYX1C1, DNAAF1, PIH1D3, SPAG1, HEATR2*) in ≈17% of families, followed by mutations in 'ruler protein' genes (*CCDC39, CCDC40*) in 16% and radial spokes (*RSPH1, RSPH3, RSPH4A, RSPH9*) in 8%. *CCDC103* mutations affected 5% families but otherwise, mutations in gene involved in ODA docking (*ARMC4, CCDC114, CCDC151*), central pair (*HYDIN*) and nexin-dynein regulatory complex structures (*CCDC65, DRC1*), multi-ciliogenesis (*CCNO, MCIDAS*) or causing 'syndromic' forms (*OFD1, RPGR*) were more rare, affecting collectively ≈9% of the families.

Overall, *DNAH5* was the most prevalent mutant gene, mutations identified in affected individuals from 27 families (21%) (**figure 1B and detailed in figure 2A**). However, populations of different ancestry (ethnicity) had considerably different genetic profiles. *DNAH5* and *DNAH11* mutations were found in 37% and 15% of European families respectively, but in only a minority of patients from other ancestries. *LRRC6* and *CCDC103* were the most frequently mutated genes in South-Asian families, affecting overall more than a third (20% and 16% respectively) of families. *CCDC39* and *CCDC40* were the major two mutant genes affecting the Arab population, identified in 42% of Arab families (**figure 1C**). As detailed further below, these frequencies were due to a mixture of recurrent, presumed founder effect mutations, as well as mutations often unique to individual families.

Expanded mutation spectrum in known PCD genes

A high proportion of families (74/128, 58%), from all ancestry groups, were found to carry homozygous variants (**figure 2B**). Surprisingly, one third of Europeans families (20/60) considered largely non-consanguineous, carry homozygous variants in known PCD genes (**online supplementary figure S3**), highlighting possible unrecognized endogamy and relatedness. Biallelic heterozygous variants in autosomal genes caused disease in 31% of patients (39 families) and in 3 families, hemizygous variants were identified in known X linked genes (*PIH1D3, RPGR, OFD1*).

Of the total of 167 variants in known PCD genes detected in the 128 families, the predominant variant types were predicted protein truncating mutations (73%) classified as frameshift 32%, nonsense 26%, and mutations affecting splicing 15%. Missense variants accounted for 21% of all variants. Copy number variations (CNV) and in-frame deletions or deletion/insertion mutations accounted for 6% of variants overall (**figure 2C**). Eleven single variants identified without a second mutation ('one hit' patients in **table S4**) were not regarded as diagnostic, but amongst the 155 variants that diagnosed 116 families (excludes *DNAH9* and *CFAP300* alleles), 82% were pathogenic (class 5) and 8% were likely pathogenic (class 4). Class 3 variants of unknown clinical significance (VUS) represented only 10% of variants; these remain under some caution for providing a definitive diagnosis (**figure 2D**).

Marked differences in the frequency and spectrum of mutations in different ancestries

Across the cohort, in addition to the presence of many family-unique mutations, the prevalence of a number of recurrent mutations presumed to reflect population bottleneck/founder effects, play a major contribution to the different genes affecting different PCD populations. We defined 14 recurrent mutations that collectively accounted for a large number of the PCD-causing variants. Some were ancestry-specific and others were present in multiple populations (**table 2**). In the 60 European families where causal alleles were defined, three recurrent *DNAH5* mutations were identified to account for 13% (16/120) of European disease alleles, two previously reported as possible founder effects (c.10815delT; p.Pro3606Hisfs*22 and c.13458_13459insT; p.Asn4487fs*1)[20-22] and a nonsense mutation (c.6261T>G; p.Tyr2087*) not previously reported (table 2, online supplementary table S3 and figure 2A). Three other previously reported mutations together accounted for another 13% (16/120) of European disease alleles: *DNAI1* c.48+2dupT; p.Ser17Valfs*12, *RSPH1* c.275-2A>C; p.Gly92Alafs*10 and a recurrent homozygous *DYX1C1* 3.5 kb genomic deletion[23-26]. *DNAH11* mutations are also a major contributor to European PCD disease, but mostly as family-unique rather than recurrent alleles.

Mutation	No. of alleles/ alleles per ancestry	No. of alleles/total alleles	Ancestry (ethnicity)	ExAc_MAF	al mena_MAF	BinB_MAF	Reported before
CCDC39 (c.1871_1872del, p.Ile624Lysfs*3)	8/48 17%	8/218 4%	Arab	Not in ExAc	Not in al mena	Not in BinB	No
RSPH9 (c.801_803delGAA, p.Lys268del)	4/48 8%	4/218 2%	Arab	0.00000576 5	3 / 0.00151	Not in BinB	Yes
DNAH5 (c.10815delT, p.Pro3606Hisfs*22)	8/120 7%	8/218 4%	European	0.0001483	Not in al mena	Not in BinB	Yes
DNAH5 (c.13458_13459insT, p.Asn4487fs*1)	5/120 4%	5/218 2%	European	0.0000578 3	Not in al mena	Not in BinB	Yes
DNAH5 (c.6261T>G, p.Tyr2087*)	3/120 2%	3/218 1%	European	Not in ExAc	Not in al mena	Not in BinB	No
DNAI1 (c.48+2dupT, p.Ser17Valfs*12)	5/120 4%	5/218 2%	European	0.0004624	Not in al mena	Not in BinB	Yes
RSPH1 (c.275-2A>C, p.Gly92Alafs*10)	7/120 6%	7/218 3%	European	0.0003625	Not in al mena	Not in BinB	Yes
DYX1C1 (3.5kb del involving exon 7)	4/120 3%	4/218 2%	European	NA	NA	NA	Yes
LRRC6 (c.630delG, p.Trp210Cysfs*12)	10/50 20%	10/218 %	South-Asian	0.000206	Not in al mena	10/0.0065	Yes
CCDC103 (c.383dup, p.Pro129Serfs*25)	4/50 8%	4/218 5%	South-Asian	Not in ExAc	Not in al mena	1/0.0006	Yes
CCDC103 (c.461A>C, p.His154Pro)	8/218 4%	8/218 4%	Multiple ancestries	0.001261	2 / 0.00101	6/0.0039	Yes
CCDC40 (c.248delC, p.Ala83Valfs*84)	4/218 2%	4/218 2%	Multiple ancestries	0.0004794	Not in al mena	Not in BinB	Yes
CCDC40 (c.2824_2825insCTGT, p.Arg942Thrfs*57)	3/218 1%	3/218 1%	Multiple ancestries	Not in ExAc	Not in al mena	Not in BinB	No
DNAH11 (c.13494_13500del, .Ser4498Argfs*15)	3/218 %	3/218 %	Multiple ancestries	Not in ExAc	Not in al mena	Not in BinB	No

Table 2. Ancestry-specific frequent mutations. No. of alleles is calculated for the 109 families in which causal alleles were identified (60 European, 25 South-Asian and 24 Arabic ancestry families). MAF, minor allele frequency; ExAc[11], Born-in-Bradford (BinB)[12] and al mena[13] databases.

In South-Asian families, a previously described *LRRC6* mutation (c.630delG; p.Trp210Cysfs*12) was the most frequent mutant allele, found in homozygous status in five South-Asian families[21]. A previously reported *CCDC103* mutation was detected in homozygous state (c.383dupG; p.Pro129Serfs*25) in two unrelated South-Asian families[22]. Together, these two variants alone accounted for 28% (14/50) of all disease alleles in the 25 South-Asian families where causal alleles were defined (**table 2 and online supplementary table S3**). A known recurrent Arabic Bedouin *RSPH9* mutation (c.801_803delGAA; p.Lys268del) was detected in homozygous state in two Arab families[23]. Another possible Arabic homozygous founder mutation (c.1871_1872delTA; p.Ile624Lysfs*3) in *CCDC39* was found in 4 Palestinian families. Together, these two variants accounted for 29% (12/48) of all disease alleles in the 24 Arabic families where causal alleles were defined (**table 2 and online supplementary table S3**). *CCDC40* mutations also contribute to Arabic PCD disease, but in the form of family-unique rather than recurrent alleles.

Of other recurrent variants, the previously reported common South-Asian *CCDC103* missense mutation (c.461A>C; p.His154Pro) was detected mostly in South-Asians, but also in European and other ancestries[18]. We also identified in different ancestries two recurrent *CCDC40* mutations, one previously reported (c.248delC; p.Ala83Valfs*84)[24, 25] and one novel (c.2824_2825insCTGT; p.Arg942Thrfs*57), in addition to one novel *DNAH11* mutation (c.13494_13500del, p.Ser4498Argfs*15).

Targeted NGS reveals synonymous variants predicted to affect splicing as a cause of PCD

We identified two synonymous coding region variants not predicted to change the encoded protein's amino acid sequence, but predicted instead to affect splicing. One in an Arab family (PCD-G086) with cilia microtubular disorganization and IDA loss, was a *CCDC40* homozygous variant (c.48A>G; p.Gly16Gly) that correctly segregated within the extended family (**online supplementary figures S4, S5**). The other in a European family (PCD-G093) with cilia ODA loss, was a *DNAH5* synonymous mutation (c.5157C>T; p.Phe1719Phe) that was combined with a missense variant (c.10815T>G; p.Asp3605Glu) (**online supplementary figures S6, S7**). Whilst it is possible these synonymous variants may affect splicing, they are currently class 3 VUS (**online supplementary table S3**) and cannot be reclassified to pathogenic or likely pathogenic without further work that provides direct observation of their presumed splicing effects.

Targeted NGS is a powerful tool for diagnosis and characterization of PCD patients

TEM analysis detected ultrastructural defects in 97/134 (72%) families. The other 37 had either normal TEM (e.g. associated with *DNAH11* and *HYDIN* defects[19, 20] or a minority of inconclusive TEM results (**table 1**). The most common ultrastructural defect was ODA loss (in 45%, 61 families), either alone (in 23%, 31 families) or combined with IDA loss (in 22%, 30 families). Other defects included microtubular disorganization with or without IDA loss (12%), central microtubular complex defects (6%), predominant isolated IDA loss (4%) or a lack of cilia (5%) (**table 1**).

We confirmed a strong correlation across the entire cohort between gene defect and expected ultrastructural defect, in agreement with the PCD literature (**tables 1 and online supplementary table S1**)[2]. Hence, TEM defects can be valuable for interpretation of genetics test results; however, the study also showed that they are not always required. For the 27/161 families (17%) without TEM data, still with strong clinical suspicion, 18 had biallelic variants in known PCD genes, hence a high proportion (67%) were confidently solved by genetics without TEM information (**online supplementary figure S8**). As a cautionary note, for a small number of patients (n=6, asterisked in **online supplementary table S3**) without a recorded TEM defect confirming of their PCD status, they also carry homozygous or biallelic heterozygous variants that are rare and in the known PCD genes, but are class 3 VUS of uncertain significance. For example PCD-G013 is biallelic heterozygous for two *DNAH5* missense changes both of unknown significance (not previously reported). In these cases, three have variants in the *HYDIN* and *DNAH11* genes associated with normal TEM (PCD-G104, -G017, -G021), but for the others the TEM could be reviewed and repeated.

To further test the power of genetic testing in the diagnostic workflow of PCD, we looked in detail at the correlation of specific PCD gene mutations with ciliary ultrastructural defects determined by TEM at a single diagnostic centre. We found that mutations in the ODA gene *DNAH5* were associated with (i) clear-cut ODA loss as expected, but also (ii) combined loss of IDA+ODA or (iii) inconclusive TEM analysis (**figure 3A; table 1**). A similar classification was possible in individuals with dynein assembly gene mutations (*LRRC6, HEATR2, DYX1C1, DNAAF3* or *DNAAF1*), where combined IDA+ODA loss is expected (**figure 3B; table 1**). By looking at the TEM data in the context of the genetic mutation, we could see a distinct pattern, since dynein assembly mutations led to combined IDA+ODA loss in most cilia cross sections,

contrasting with *DNAH5* mutations causing mainly ODA loss. Therefore, genetic data allows these two categories of genetically diagnosed patients to be distinguished (**figure 3**).

DISCUSSION

There is high underlying disease heterogeneity and no gold standard test available yet to exclude PCD, so a combination of tests interpreted in the light of clinical symptoms tends to be used for diagnosis. This increasingly includes genetic analysis[8]. Here, the utility of genetic screening was evaluated in a large cohort of 161 unrelated PCD families from various ancestries including European, Arab and South-Asian, by NGS screening with additional CNV analysis of the known PCD genes and a panel of other candidate genes. This gave a high yield of a confirmed or highly suggested PCD diagnosis in 75% of families. A further 7% of families with single heterozygous variants in known PCD genes that looked likely causal likely may carry a second mutation that NGS was not able to detect, for example a deep intronic variant.

The identification of clear-cut ciliary ultrastructural defects by TEM analysis remains a confirmatory step in the PCD diagnostic workflow, although failure to identify TEM defects does not exclude PCD[8]. Here, we identified mutations in known PCD genes in 81% of patients with normal or inconclusive TEM findings, implying significant potential for incorporating genetics earlier within the diagnostic pipeline, as previously discussed[19]. We could also diagnose 67% of patients with a strong history where TEM was not available, as well as other difficult cases e.g. *CCDC103* p.His154Pro mutations, where other tests often give equivocal results[18].

19

Our diagnostic output is higher than most previous NGS targeted panel screens in PCD[26-29], similar to the 76% diagnostic success achieved from WES and targeted CNV analysis in 52 individuals[30, 31]. The limitations include the unknown genes that are absent from the panel, the incomplete genetic diagnosis when variants of uncertain significance or single heterozygous variants in PCD genes are detected, technical issues affecting sequence coverage depth, the known bioinformatics challenges to identify CNVs[32] and a well-known problem with identification of *HYDIN* mutations, due to the *HYDIN2* copy gene[20].

This study expands the genetic landscape and mutation spectrum of PCD by identifying 61 previously reported and 88 previously unrecognized variants, hence 57% of all the variants classified here as likely pathogenic are novel (**online supplementary table S3**). Most were protein truncating mutations, consistent with previous reports. Synonymous mutations are not commonly reported in PCD, but we identified two predicted to result in alteration of splicing, raising the importance of looking for potential synonymous variants in unsolved cases.

In agreement with previous studies, most of the identified PCD variants were private[1, 8], however several were detected in more than one unrelated family that tended to be more frequent in certain populations. Interestingly, one third of mutations in European families were homozygous despite the low recorded European consanguinity rate, with only one European family reporting consanguineous marriage. In 14 European families, their identified mutations were reported before in the literature, suggesting they may reflect European founder effects. Overall, we found that *DNAH5* is the most commonly mutated PCD gene in agreement with other studies[33], but this was not the case in all ancestries. We identified *DNAH5* mutations in 37% of European families, representing the most common mutant gene in Europeans. In

contrast, *LRRC6* and *CCDC103* mutations were more prevalent in South-Asian families amongst whom we found only one family with *DNAH5* mutations. In Arab families, *DNAH5* mutations were identified in only two families, with *CCDC39*, *CCDC40* and *RSPH9* mutations much more prevalent.

The study has therefore uncovered a striking population-based genetic stratification underlying PCD. It highlights the impact of ancestry upon the genetics of PCD and the importance of including patients from various ancestries to elucidate the full genetic landscape of PCD. This information is diagnostically relevant, as it could be used for improved, smaller/cheaper carrier screening panels targeting certain populations and preliminary allelic-specific genetic diagnosis by Sanger sequencing, especially in countries where NGS facilities are not widely available. The clinical relevance of genetic disease stratification remains poorly understood, but more studies are emerging with PCD genotype-phenotype correlations which can increasingly impact upon disease management[4, 34-36].

Although we could confirm good correlation between genotype and cilia ultrastructural phenotype, some differences in the TEM analysis results were evident even with mutations in the same gene. *DNAH5* mutations were associated with ODA loss in the majority of cases but also with inconclusive TEM results, possibly due to difficulties in evaluating IDA by TEM[3, 8], as well as with combined IDA+ODA loss that is more often linked to dynein assembly gene mutations. Quantification of the percentage of arm loss arising from *DNAH5* mutations compared to mutations in dynein assembly genes showed that augmenting TEM data with genetics could clearly distinguish these two groups, *DNAH5* mutations being more highly

linked to ODA loss and dynein assembly mutations more highly to combined IDA and ODA loss.

In conclusion, targeted multi-gene panel sequencing is a cost-effective, time efficient single test which in this study diagnosed around 75% of PCD cases. It improves the diagnostic workflow outcome, confirming PCD in patients with inconclusive TEM results and helping in diagnosis of patients where TEM analysis is not available. The sensitivity (diagnostic yield) of gene tests for PCD will continue to increase with gene discovery progress. *CFAP300, DNAH9, GAS2L2, LRRC56, MNS1, DNAH1, DNAH6* are all genes that have become associated with PCD or confirmed as PCD genes, in the interim study period[16, 17, 37-41]. Despite the current incomplete PCD gene list, this strongly supports the importance of including genetics into the diagnostic pathway where it can play a key role, overcoming the pitfalls of other diagnostic measures. This may be particularly relevant in countries where access to other specialized PCD tests is not available. Major impact genes and recurrent mutations have emerged in this study, in addition to a notable impact of ancestry on the genetic variability of PCD, which has implications for the improved stratification of PCD patients to help facilitate better targeting of diagnostics and disease management.

CONTRIBUTORSHIP STATEMENT

MRF, MPP, TC, JH, LJ, DM-R, CMW, HM and HMM performed genetic and bioinformatic analysis and analysed genetics data. AS, MD, AVR, SO, CJ, PG, RAH, AR, JT, AP and SL were involved in generating and analysing clinical functional tests. AS, MD, AVR, PG, AR and AP performed cilia ultrastructural analysis. MRF, PA, EM, PC, CO'C, RW, SC, WW, HM, WS, LP, CC, MRL, EMKC, PK, NR, NF, JSL, CH and HMM ascertained patients and acquired patient data and samples. HMM conceived and supervised the study and data interpretation. MRF interpreted the genetics data, developed the manuscript draft and generated the figures. MRF and HMM wrote the manuscript with critical review input from AS, TC, CMW, JSL and CH. All authors reviewed and approved the final manuscript.

FUNDING

COMPETING INTERESTS

The authors declare that they have no competing interests.

ACKNOWLEDGEMENTS

REFERENCES

1.   A. Horani, T. W. Ferkol, S. K. Dutcher and S. L. Brody. Genetics and biology of primary ciliary dyskinesia. *Paediatr Respir Rev* 2016;**18**:18-24.

2.   H. M. Mitchison and E. M. Valente. Motile and non-motile cilia in human pathology: from function to phenotypes. *J Pathol* 2016.

3.   J. S. Lucas, A. Burgess, H. M. Mitchison, E. Moya, M. Williamson, C. Hogg and U. K. National PCD Service. Diagnosis and management of primary ciliary dyskinesia. *Archives of disease in childhood* 2014;**99**(9):850-6.

4.   I. Amirav, J. Wallmeier, N. T. Loges, T. Menchen, P. Pennekamp, H. Mussaffi, R. Abitbul, A. Avital, L. Bentur, G. W. Dougherty, E. Nael, M. Lavie, H. Olbrich, C. Werner, C. Kintner, H. Omran and P. C. D. C. I. Israeli. Systematic Analysis of CCNO Variants in a Defined Population: Implications for Clinical Phenotype and Differential Diagnosis. *Hum Mutat* 2016;**37**(4):396-405.

5.   M. Boon, J. Wallmeier, L. Ma, N. T. Loges, M. Jaspers, H. Olbrich, G. W. Dougherty, J. Raidt, C. Werner, I. Amirav, A. Hevroni, R. Abitbul, A. Avital, R. Soferman, M. Wessels, C. O'Callaghan, E. M. Chung, A. Rutman, R. A. Hirst, E. Moya, H. M. Mitchison, S. Van Daele, K. De Boeck, M. Jorissen, C. Kintner, H. Cuppens and H. Omran. MCIDAS mutations result in a mucociliary clearance disorder with reduced generation of multiple motile cilia. *Nat Commun* 2014;**5**:4418.

6.   C. E. Kuehni, T. Frischer, M. P. Strippoli, E. Maurer, A. Bush, K. G. Nielsen, A. Escribano, J. S. Lucas, P. Yiallouros, H. Omran, E. Eber, C. O'Callaghan, D. Snijders, A. Barbato and E. R. S. T. F. o. P. C. D. i. Children. Factors influencing age at diagnosis of primary ciliary dyskinesia in European children. *The European respiratory journal* 2010;**36**(6):1248-58.

7.   A. J. Shapiro, M. A. Zariwala, T. Ferkol, S. D. Davis, S. D. Sagel, S. D. Dell, M. Rosenfeld, K. N. Olivier, C. Milla, S. J. Daniel, A. J. Kimple, M. Manion, M. R. Knowles and M. W. Leigh.

Diagnosis, monitoring, and treatment of primary ciliary dyskinesia: PCD foundation consensus recommendations based on state of the art review. *Pediatr Pulmonol* 2016;**51**(2):115-32.

8.   J. S. Lucas, A. Barbato, S. A. Collins, M. Goutaki, L. Behan, D. Caudri, S. Dell, E. Eber, E. Escudier, R. A. Hirst, C. Hogg, M. Jorissen, P. Latzin, M. Legendre, M. W. Leigh, F. Midulla, K. G. Nielsen, H. Omran, J. F. Papon, P. Pohunek, B. Redfern, D. Rigau, B. Rindlisbacher, F. Santamaria, A. Shoemark, D. Snijders, T. Tonia, A. Titieni, W. T. Walker, C. Werner, A. Bush and C. E. Kuehni. European Respiratory Society guidelines for the diagnosis of primary ciliary dyskinesia. *The European respiratory journal* 2017;**49**(1).

9.   A. Grada and K. Weinbrecht. Next-generation sequencing: methodology and application. *J Invest Dermatol* 2013;**133**(8):e11.

10. E. Omoyinmi, A. Standing, A. Keylock, F. Price-Kuehne, S. Melo Gomes, D. Rowczenio, S. Nanthapisal, T. Cullup, R. Nyanhete, E. Ashton, C. Murphy, M. Clarke, H. Ahlfors, L. Jenkins, K. Gilmour, D. Eleftheriou, H. J. Lachmann, P. N. Hawkins, N. Klein and P. A. Brogan. Clinical impact of a targeted next-generation sequencing gene panel for autoinflammation and vasculitis. *PLoS One* 2017;**12**(7):e0181874.

11. M. Lek, K. J. Karczewski, E. V. Minikel, K. E. Samocha, E. Banks, T. Fennell, A. H. O'Donnell-Luria, J. S. Ware, A. J. Hill, B. B. Cummings, T. Tukiainen, D. P. Birnbaum, J. A. Kosmicki, L. E. Duncan, K. Estrada, F. Zhao, J. Zou, E. Pierce-Hoffman, J. Berghout, D. N. Cooper, N. Deflaux, M. DePristo, R. Do, J. Flannick, M. Fromer, L. Gauthier, J. Goldstein, N. Gupta, D. Howrigan, A. Kiezun, M. I. Kurki, A. L. Moonshine, P. Natarajan, L. Orozco, G. M. Peloso, R. Poplin, M. A. Rivas, V. Ruano-Rubio, S. A. Rose, D. M. Ruderfer, K. Shakir, P. D. Stenson, C. Stevens, B. P. Thomas, G. Tiao, M. T. Tusie-Luna, B. Weisburd, H. H. Won, D. Yu, D. M. Altshuler, D. Ardissino, M. Boehnke, J. Danesh, S. Donnelly, R. Elosua, J. C. Florez, S. B. Gabriel, G. Getz, S. J. Glatt, C. M. Hultman, S. Kathiresan, M. Laakso, S. McCarroll, M. I. McCarthy, D. McGovern, R. McPherson, B. M. Neale, A. Palotie, S. M. Purcell, D. Saleheen, J. M. Scharf, P. Sklar, P. F. Sullivan, J. Tuomilehto, M. T. Tsuang, H. C. Watkins, J. G. Wilson,

M. J. Daly, D. G. MacArthur and C. Exome Aggregation. Analysis of protein-coding genetic variation in 60,706 humans. *Nature* 2016;**536**(7616):285-91.

12.　E. Sheridan, J. Wright, N. Small, P. C. Corry, S. Oddie, C. Whibley, E. S. Petherick, T. Malik, N. Pawson, P. A. McKinney and R. C. Parslow. Risk factors for congenital anomaly in a multiethnic birth cohort: an analysis of the Born in Bradford study. *Lancet* 2013;**382**(9901):1350-9.

13.　R. Koshy, A. Ranawat and V. Scaria. al mena: a comprehensive resource of human genetic variants integrating genomes and exomes from Arab, Middle Eastern and North African populations. *J Hum Genet* 2017;**62**(10):889-94.

14.　S. Richards, N. Aziz, S. Bale, D. Bick, S. Das, J. Gastier-Foster, W. W. Grody, M. Hegde, E. Lyon, E. Spector, K. Voelkerding, H. L. Rehm and A. L. Q. A. Committee. Standards and guidelines for the interpretation of sequence variants: a joint consensus recommendation of the American College of Medical Genetics and Genomics and the Association for Molecular Pathology. *Genet Med* 2015;**17**(5):405-24.

15.　V. Plagnol, J. Curtis, M. Epstein, K. Y. Mok, E. Stebbings, S. Grigoriadou, N. W. Wood, S. Hambleton, S. O. Burns, A. J. Thrasher, D. Kumararatne, R. Doffinger and S. Nejentsev. A robust model for read count data in exome sequencing experiments and implications for copy number variant calling. *Bioinformatics* 2012;**28**(21):2747-54. 6.

16.　M. R. Fassad, A. Shoemark, P. le Borgne, F. Koll, M. Patel, M. Dixon, J. Hayward, C. Richardson, E. Frost, L. Jenkins, T. Cullup, E. M. K. Chung, M. Lemullois, A. Aubusson-Fleury, C. Hogg, D. R. Mitchell, A. M. Tassin and H. M. Mitchison. C11orf70 Mutations Disrupting the Intraflagellar Transport-Dependent Assembly of Multiple Axonemal Dyneins Cause Primary Ciliary Dyskinesia. *Am J Hum Genet* 2018;**102**(5):956-72.

17.　M. R. Fassad, A. Shoemark, M. Legendre, R. A. Hirst, F. Koll, P. le Borgne, B. Louis, F. Daudvohra, M. P. Patel, L. Thomas, M. Dixon, T. Burgoyne, J. Hayes, A. G. Nicholson, T. Cullup, L. Jenkins, S. B. Carr, P. Aurora, M. Lemullois, A. Aubusson-Fleury, J. F. Papon, C.

O'Callaghan, S. Amselem, C. Hogg, E. Escudier, A. M. Tassin and H. M. Mitchison. Mutations in Outer Dynein Arm Heavy Chain DNAH9 Cause Motile Cilia Defects and Situs Inversus. *Am J Hum Genet* 2018;**103**(6):984-94.

18. A. Shoemark, E. Moya, R. A. Hirst, M. P. Patel, E. A. Robson, J. Hayward, J. Scully, M. R. Fassad, W. Lamb, M. Schmidts, M. Dixon, R. S. Patel-King, A. V. Rogers, A. Rutman, C. L. Jackson, P. Goggin, B. Rubbo, S. Ollosson, S. Carr, W. Walker, B. Adler, M. R. Loebinger, R. Wilson, A. Bush, H. Williams, C. Boustred, L. Jenkins, E. Sheridan, E. M. K. Chung, C. M. Watson, T. Cullup, J. S. Lucas, P. Kenia, C. O'Callaghan, S. M. King, C. Hogg and H. M. Mitchison. High prevalence of CCDC103 p.His154Pro mutation causing primary ciliary dyskinesia disrupts protein oligomerisation and is associated with normal diagnostic investigations. *Thorax* 2018;**73**(2):157-66.

19. M. R. Knowles, M. W. Leigh, J. L. Carson, S. D. Davis, S. D. Dell, T. W. Ferkol, K. N. Olivier, S. D. Sagel, M. Rosenfeld, K. A. Burns, S. L. Minnix, M. C. Armstrong, A. Lori, M. J. Hazucha, N. T. Loges, H. Olbrich, A. Becker-Heck, M. Schmidts, C. Werner, H. Omran, M. A. Zariwala and C. Genetic Disorders of Mucociliary Clearance. Mutations of DNAH11 in patients with primary ciliary dyskinesia with normal ciliary ultrastructure. *Thorax* 2012;**67**(5):433-41.

20. H. Olbrich, M. Schmidts, C. Werner, A. Onoufriadis, N. T. Loges, J. Raidt, N. F. Banki, A. Shoemark, T. Burgoyne, S. Al Turki, M. E. Hurles, U. K. Consortium, G. Kohler, J. Schroeder, G. Nurnberg, P. Nurnberg, E. M. Chung, R. Reinhardt, J. K. Marthin, K. G. Nielsen, H. M. Mitchison and H. Omran. Recessive HYDIN mutations cause primary ciliary dyskinesia without randomization of left-right body asymmetry. *Am J Hum Genet* 2012;**91**(4):672-84.

21. M. A. Zariwala, H. Y. Gee, M. Kurkowiak, D. A. Al-Mutairi, M. W. Leigh, T. W. Hurd, R. Hjeij, S. D. Dell, M. Chaki, G. W. Dougherty, M. Adan, P. C. Spear, J. Esteve-Rudd, N. T. Loges, M. Rosenfeld, K. A. Diaz, H. Olbrich, W. E. Wolf, E. Sheridan, T. F. Batten, J. Halbritter, J. D. Porath, S. Kohl, S. Lovric, D. Y. Hwang, J. E. Pittman, K. A. Burns, T. W. Ferkol, S. D. Sagel, K. N. Olivier, L. C. Morgan, C. Werner, J. Raidt, P. Pennekamp, Z. Sun,

W. Zhou, R. Airik, S. Natarajan, S. J. Allen, I. Amirav, D. Wieczorek, K. Landwehr, K. Nielsen, N. Schwerk, J. Sertic, G. Kohler, J. Washburn, S. Levy, S. Fan, C. Koerner-Rettberg, S. Amselem, D. S. Williams, B. J. Mitchell, I. A. Drummond, E. A. Otto, H. Omran, M. R. Knowles and F. Hildebrandt. ZMYND10 is mutated in primary ciliary dyskinesia and interacts with LRRC6. *Am J Hum Genet* 2013;**93**(2):336-45.

22. J. R. Panizzi, A. Becker-Heck, V. H. Castleman, D. A. Al-Mutairi, Y. Liu, N. T. Loges, N. Pathak, C. Austin-Tse, E. Sheridan, M. Schmidts, H. Olbrich, C. Werner, K. Haffner, N. Hellman, R. Chodhari, A. Gupta, A. Kramer-Zucker, F. Olale, R. D. Burdine, A. F. Schier, C. O'Callaghan, E. M. Chung, R. Reinhardt, H. M. Mitchison, S. M. King, H. Omran and I. A. Drummond. CCDC103 mutations cause primary ciliary dyskinesia by disrupting assembly of ciliary dynein arms. *Nat Genet* 2012;**44**(6):714-9.

23. M. M. Alsaadi, T. R. Gaunt, C. R. Boustred, P. A. Guthrie, X. Liu, L. Lenzi, L. Rainbow, N. Hall, K. K. Alharbi and I. N. Day. From a single whole exome read to notions of clinical screening: primary ciliary dyskinesia and RSPH9 p.Lys268del in the Arabian Peninsula. *Ann Hum Genet* 2012;**76**(3):211-20.

24. D. Antony, A. Becker-Heck, M. A. Zariwala, M. Schmidts, A. Onoufriadis, M. Forouhan, R. Wilson, T. Taylor-Cox, A. Dewar, C. Jackson, P. Goggin, N. T. Loges, H. Olbrich, M. Jaspers, M. Jorissen, M. W. Leigh, W. E. Wolf, M. L. Daniels, P. G. Noone, T. W. Ferkol, S. D. Sagel, M. Rosenfeld, A. Rutman, A. Dixit, C. O'Callaghan, J. S. Lucas, C. Hogg, P. J. Scambler, R. D. Emes, Uk10k, E. M. Chung, A. Shoemark, M. R. Knowles, H. Omran and H. M. Mitchison. Mutations in CCDC39 and CCDC40 are the major cause of primary ciliary dyskinesia with axonemal disorganization and absent inner dynein arms. *Hum Mutat* 2013;**34**(3):462-72.

25. A. Becker-Heck, I. E. Zohn, N. Okabe, A. Pollock, K. B. Lenhart, J. Sullivan-Brown, J. McSheene, N. T. Loges, H. Olbrich, K. Haeffner, M. Fliegauf, J. Horvath, R. Reinhardt, K. G. Nielsen, J. K. Marthin, G. Baktai, K. V. Anderson, R. Geisler, L. Niswander, H. Omran and R.

D. Burdine. The coiled-coil domain containing protein CCDC40 is essential for motile cilia function and left-right axis formation. *Nat Genet* 2011;**43**(1):79-84.

26. F. Boaretto, D. Snijders, C. Salvoro, A. Spalletta, M. L. Mostacciuolo, M. Collura, S. Cazzato, D. Girosi, M. Silvestri, G. A. Rossi, A. Barbato and G. Vazza. Diagnosis of Primary Ciliary Dyskinesia by a Targeted Next-Generation Sequencing Panel: Molecular and Clinical Findings in Italian Patients. *J Mol Diagn* 2016;**18**(6):912-22.

27. M. Andjelkovic, P. Minic, M. Vreca, M. Stojiljkovic, A. Skakic, A. Sovtic, M. Rodic, V. Skodric-Trifunovic, N. Maric, J. Visekruna, V. Spasovski and S. Pavlovic. Genomic profiling supports the diagnosis of primary ciliary dyskinesia and reveals novel candidate genes and genetic variants. *PLoS One* 2018;**13**(10):e0205422..

28. J. Djakow, L. Kramna, L. Dusatkova, J. Uhlik, J. P. Pursiheimo, T. Svobodova, P. Pohunek and O. Cinek. An effective combination of sanger and next generation sequencing in diagnostics of primary ciliary dyskinesia. *Pediatr Pulmonol* 2016;**51**(5):498-509.

29. T. Paff, I. E. Kooi, Y. Moutaouakil, E. Riesebos, E. A. Sistermans, H. Daniels, J. M. M. Weiss, H. Niessen, E. G. Haarman, G. Pals and D. Micha. Diagnostic yield of a targeted gene panel in primary ciliary dyskinesia patients. *Hum Mutat* 2018;**39**(5):653-65.

30. R. H. Kim, A. H. D, E. Cutz, M. R. Knowles, K. A. Nelligan, K. Nykamp, M. A. Zariwala and S. D. Dell. The role of molecular genetic analysis in the diagnosis of primary ciliary dyskinesia. *Ann Am Thorac Soc* 2014;**11**(3):351-9..

31. C. R. Marshall, S. W. Scherer, M. A. Zariwala, L. Lau, T. A. Paton, T. Stockley, R. K. Jobling, P. N. Ray, M. R. Knowles, D. A. Hall, S. D. Dell and R. H. Kim. Whole-Exome Sequencing and Targeted Copy Number Analysis in Primary Ciliary Dyskinesia. *G3 (Bethesda)* 2015;**5**(8):1775-81.

32. C. Gonzaga-Jauregui, J. R. Lupski and R. A. Gibbs. Human genome sequencing in health and disease. *Annual review of medicine* 2012;**63**:35-61.

33.   J. Raidt, J. Wallmeier, R. Hjeij, J. G. Onnebrink, P. Pennekamp, N. T. Loges, H. Olbrich, K. Haffner, G. W. Dougherty, H. Omran and C. Werner. Ciliary beat pattern and frequency in genetic variants of primary ciliary dyskinesia. *The European respiratory journal* 2014;**44**(6):1579-88.

34.   S. Irving, M. Dixon, M. R. Fassad, E. Frost, J. Hayward, K. Kilpin, S. Ollosson, A. Onoufriadis, M. P. Patel, J. Scully, S. B. Carr, H. M. Mitchison, M. R. Loebinger, C. Hogg, A. Shoemark and A. Bush. Primary Ciliary Dyskinesia Due to Microtubular Defects is Associated with Worse Lung Clearance Index. *Lung* 2018;**196**(2):231-38.

35.   M. R. Knowles, L. E. Ostrowski, M. W. Leigh, P. R. Sears, S. D. Davis, W. E. Wolf, M. J. Hazucha, J. L. Carson, K. N. Olivier, S. D. Sagel, M. Rosenfeld, T. W. Ferkol, S. D. Dell, C. E. Milla, S. H. Randell, W. Yin, A. Sannuti, H. M. Metjian, P. G. Noone, P. J. Noone, C. A. Olson, M. V. Patrone, H. Dang, H. S. Lee, T. W. Hurd, H. Y. Gee, E. A. Otto, J. Halbritter, S. Kohl, M. Kircher, J. Krischer, M. J. Bamshad, D. A. Nickerson, F. Hildebrandt, J. Shendure and M. A. Zariwala. Mutations in RSPH1 cause primary ciliary dyskinesia with a unique clinical and ciliary phenotype. *American journal of respiratory and critical care medicine* 2014;**189**(6):707-17.

36.   S. D. Davis, T. W. Ferkol, M. Rosenfeld, H. S. Lee, S. D. Dell, S. D. Sagel, C. Milla, M. A. Knowles and M. W. Leigh. Clinical features of childhood primary ciliary dyskinesia by genotype and ultrastructural phenotype. *American journal of respiratory and critical care medicine* 2015;**191**(3):316-24.

37.   X. M. Bustamante-Marin, W. N. Yin, P. R. Sears, M. E. Werner, E. J. Brotslaw, B. J. Mitchell, C. M. Jania, K. L. Zeman, T. D. Rogers, L. E. Herring, L. Refabert, L. Thomas, S. Amselem, E. Escudier, M. Legendre, B. R. Grubb, M. R. Knowles, M. A. Zariwala and L. E. Ostrowski. Lack of GAS2L2 Causes PCD by Impairing Cilia Orientation and Mucociliary Clearance. *Am J Hum Genet* 2019;**104**(2):229-45.

38. S. Bonnefoy, C. M. Watson, K. D. Kernohan, M. Lemos, S. Hutchinson, J. A. Poulter, L. A. Crinnion, I. Berry, J. Simmonds, P. Vasudevan, C. O'Callaghan, R. A. Hirst, A. Rutman, L. Huang, T. Hartley, D. Grynspan, E. Moya, C. Li, I. M. Carr, D. T. Bonthron, M. Leroux, C. Care4Rare Canada, K. M. Boycott, P. Bastin and E. G. Sheridan. Biallelic Mutations in LRRC56, Encoding a Protein Associated with Intraflagellar Transport, Cause Mucociliary Clearance and Laterality Defects. *Am J Hum Genet* 2018;**103**(5):727-39.

39. A. Ta-Shma, R. Hjeij, Z. Perles, G. W. Dougherty, I. Abu Zahira, S. J. F. Letteboer, D. Antony, A. Darwish, D. A. Mans, S. Spittler, C. Edelbusch, S. Cindric, T. Nothe-Menchen, H. Olbrich, F. Stuhlmann, I. Aprea, P. Pennekamp, N. T. Loges, O. Breuer, A. Shaag, A. Rein, E. Y. Gulec, A. Gezdirici, R. Abitbul, N. Elias, I. Amirav, M. Schmidts, R. Roepman, O. Elpeleg and H. Omran. Homozygous loss-of-function mutations in MNS1 cause laterality defects and likely male infertility. *PLoS Genet* 2018;**14**(8):e1007602.

40. F. Imtiaz, R. Allam, K. Ramzan and M. Al-Sayed. Variation in DNAH1 may contribute to primary ciliary dyskinesia. *BMC Med Genet* 2015;**16**:14.

41. Y. Li, H. Yagi, E. O. Onuoha, R. R. Damerla, R. Francis, Y. Furutani, M. Tariq, S. M. King, G. Hendricks, C. Cui, M. Saydmohammed, D. M. Lee, M. Zahid, I. Sami, L. Leatherbury, G. J. Pazour, S. M. Ware, T. Nakanishi, E. Goldmuntz, M. Tsang and C. W. Lo. DNAH6 and Its Interactions with PCD Genes in Heterotaxy and Primary Ciliary Dyskinesia. *PLoS Genet* 2 016;**12**(2):e1005821.

Figure legends

Figure 1. Targeted next generation sequencing yields a high (72%) diagnostic output in PCD patients and reveals a diverse mutation landscape stratified by ancestry

A, Flow chart of genetic results found for families enrolled in the study describing the genetic diagnostic output. Probands from 161 unrelated families were subject to next generation sequencing using a multi-gene motile ciliome panel. Affected individuals in four of the 13 'candidate gene' families carried biallelic variants in two genes now recognized as disease-casing, *CFAP300* and *DNAH9*, see main text for details. B, The genetic stratification of all 161 from the multi-ancestry cohort found to carry mutations in known PCD genes. C, Summary of mutated genes in three different populations illustrating that different ancestries have different genetics. Amongst 109 European, Arabic and South Asian families, the genes most commonly detected to carry mutations are *DNAH5* in European families (37%), *LRRC6* and *CCDC103* in South-Asian families (36%) and *CCDC39* and *CCDC40* in Arabic families (42%).

Figure 2. PCD-causing mutation distribution in the multi-ancestry cohort is dominated by protein truncating and homozygous mutations

A, Schematic of the *DNAH5* mutations identified in this study, marked in yellow if previously reported. Recurrent mutations are boxed in bold. Conserved domains of the DNAH5 protein are indicated on the genomic structure. Variants are numbered according to (NM_001369.2) transcript. B, Families with mutations in known PCD genes grouped based on their zygosity status showed that about 58% of mutations identified in this study were present in patients in a homozygous state. C, Mutations classified according to their

impact on the respective proteins showed that frameshift and nonsense mutations were the most prevalent (58%) with 15% splicing defects and 21% missense changes. Collectively, mutations predicted to have a protein truncating effect represent about 77% (frameshift, nonsense, splicing defects and CNVs). D, Mutations identified in biallelic state in autosomal gene or hemizygous state in X-linked gene classified based on the guidelines from the American College of Medical Genetics showed that 82% of mutations were class 5 (clearly pathogenic), 8% class 4 (likely pathogenic) and 10% class 3 (uncertain significance).

Figure 3. Genetics can better characterize PCD patients and overcome other diagnostic testing inconsistencies

For a selected set of patients, the percentage of cilia cross sections showing a loss of either or both the inner and outer dynein arms was recorded in the routine TEM diagnostic setting at Royal Brompton Hospital with reference to the underlying genetic defects. a) Patients carrying biallelic mutations in outer dynein arm components showed mainly an isolated loss of outer dynein arms. Combined IDA+ODA loss was also noted. Interesting, quite variable numbers of cross sections showed a normal ultrastructure of the cilia. b) Patients carrying biallelic mutations in dynein assembly genes showed a combined loss of both arms in the majority of cross sections examined. Variable isolated arm loss was also reported.

Extended Reality Approach for Construction Quality Control

Mustafa Al-Adhami,
University of Huddersfield
(Email: Mus.adhami@hud.ac.uk)
Song Wu,
University of Huddersfield
(Email: S.Wu@hud.ac.uk)
Ling Ma,
University College London
(Email: l.ma@ucl.ac.uk)

Abstract

Inspection is one of the most important factors in quality management. Neglecting inspection process may cause construction errors, quality degradation, and unnecessary expenses. Quality management is performed by the site manager to ensure construction work specifications are implemented according to the design. The conventional method of construction site inspection required site manager to record information about the defect in documents manually (e.g., checklist, drawings) and then re-entered this information into the company server. Furthermore, this process depends mainly on the inspector's skill which may be inefficient and time-consuming. This study aims to leverage the quality control and site inspection process with the overall objective of reducing major error and extra costs using BIM-based extended reality.

The recent advancement of extended reality technology has shown the potential of being the future visualization tool of the AEC/FM industry. The visualization capability of this technology to retrieve virtual models and other related built environment data in a real-world environment and overlaid the existing building structure can enhance the quality of inspection. However, there are many challenges associated with the implementing of extended reality technology and its efficiency in a real workplace. In this paper, the implementation and the feasibility of BIM-based XR technology for quality control inspection have been investigated and discussed based on an experiment on a real construction site.

Keywords: Augmented reality, BIM, Quality control, Inspection, Built environment

1. Introduction

In the construction field, quality control (QC) inspection is taking place after specific work packages are completed to ensure the construction work is following design specifications. In most cases, the site manager is responsible for audit and record information about the defect in construction manually based on a checklist and drawings and then generate a reported with all issues that need to be discussed among project stockholders. This process depends on the inspector's skill of extracting the necessary information from design and compare it with the as-built which might be inefficient and time-consuming. Recently there are many efforts in the BE to improve this process especially with the latest advancement in digitalization.

In the last decade, the built environment (BE) witnessed a significant improvement in digitalization, converting building information into a digital format (Chu et al., 2018), building information modeling (BIM) has started to become the official form of the BE. The use of BIM has allowed project parties to obtain project information and relevant data all integrated into three-dimensional (3D) digital form. The benefits brought by BIM have been reported in several areas and different stages of a project life cycle (Zhao, 2017). However, the execution of BIM to support construction site activities is associated with many difficulties such as how to bring BIM outside the office environment.

Obviously, BIM is not just a 3D model technology, but it is also advanced project documentation, it includes information like geo-location, spatial data, and construction schedule, yet, the implementation of BIM for on-site operation still depends on printed drawings or portable devices with BIM viewer. This approach has several limitations, 1) The user of BIM viewer needs to do manual operations to reach the required information, such as navigation, cross-section, hiding components; 2) difficulty to show the model based on user location on-site; 3) Moreover, the construction crew still prefers the conventional method, 2D projection drawings, to extract design situation and draw them directly on the workspace. Thus, any misinterpretation to the design information might lead to construction error which is costly in time and resources. Accordingly, the level of interaction between BIM and construction environment is extremely week, which might hinder the grasp of project information and limits the integration of BIM for on-site job task (Wang et al., 2014).

The recent advancement of extended reality (XR) technologies has been explored by many applications in the BE, such as virtual reality (VR) for design review (Maftei and Harty, 2015), training (Bosché et al., 2016), augmented reality for construction assembly (Wang et al., 2014), and so on. Augmented reality (AR) is an enhanced version of reality where the user is able to visualize and interact with virtual contents in the real environment (Wang et al., 2016). Although AR technology appears to be a promising medium to improve communication and integration of construction crew with BIM, the usability and effectiveness of this technology have not been proved (Wang et al., 2013). Additionally, the number of studies investigate proof of the benefits of AR to enhance construction tasks are limited (Meža et al., 2014). Since BIM and AR are complementary technologies (Wang et al., 2013), the available research in the BE domain demonstrates numerous frameworks of integration using many technologies in hardware and software, most of them examined BIM-AR integration from a technical perspective only. Hence, there is a need for sufficient insight into how that might work on a real job site.

AR studies in construction domain focused on the system development process rather than validate the application approach on the hand of end users (Wang et al., 2013). Nowadays, many AR systems are available, AR headset like a Magic leap, Hololens and Meta 2, BIM AR plugins like Trimble Connect and VisualLive. The application development is different for each device, but the concept is still the same. Therefore, this study decided to investigate the feasibility and practicality of AR technology as a concept for QC inspection. It has to mention this study is aware of the level of maturity of the current AR devices and the developing tool as this can affect the overall AR experience and lead to false validation results.

To this end, the current study has utilized the conventional role of AR technologies to visualize design

data that feed into the AR headset and give the inspector easy access to specific type of information that can enhance his or her reality to do the required task. BIM has been used as a primary source of delivering the necessary information for the inspector, such as geometries, dimensions, and component properties. There are several technical challenges associated with the integration of BIM and AR technology have investigated like the complexity of the model, data format, the processing capability of AR devices. Nevertheless, this study aims to demonstrate on a job-site a smooth and sufficient AR experience that can enable the site manager to retrieve design information on the construction environment.

2. XR Applications in Construction

Extended reality is a term used to describe the whole spectrum of simulated reality technologies, starting from the real environment to completely virtual see *Figure 26*. XR applications first introduced to the public in the 90s, however, it wasn't mature enough for adoption (Steinicke, 2016). In recent years, XR technologies have started to span many fields such as education (Freina and Ott, 2015), healthcare (Huang et al., 2018, Kim et al., 2017b), cultural heritage (Bekele et al., 2018), military (Page, 2000, Delaney, 2014), in fact, any domain relies on digital graphics can benefits from the visualization capability of this technology (Linowes, 2015). Today, the BE has a significant improvement in the digitalization, the benefits of BIM become clearer (Drettakis et al., 2007). Cloud computing capabilities have leveraged communication and information exchange among stakeholders. Portable smart technologies provide easy access to up-to-date building information (e.g., plans, schedules, budgets) anytime anywhere. Although there are many positive aspects of digitalization, a huge concern raised about its impact on workers productivity (Agarwala, 2014), as they might be exposed to a significant amount of data that required more time to manipulate or managing the data. Consequently, they will confront the complexity of the system, rather than gain its potential benefits (Aral et al., 2012, Chu et al., 2018).
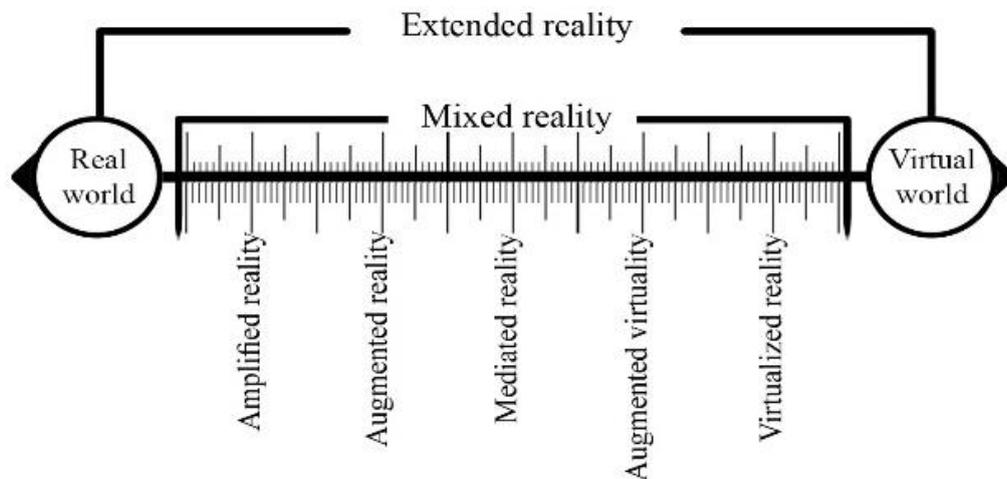
Figure 26: extended reality (XR) spectrum

A growing number of studies has started exploring the visualization capability of AR technology, as it has appeared to be a promising medium to improve several activities in the construction domain (Li et al., 2018, Jennifer Whyte, 2018). In the last five years, the research community in the construction domain has presented several studies exploring AR applications to support fieldwork, handheld devices (i.e., smartphones, tablets) has been used widely in their studies. For the purpose of construction monitoring, the integration of BIM and AR has been investigated by (Meža et al., 2014) to enable the project manager to follow up with the planned schedules, while (Zaher et al., 2018) integrate 5D BIM and AR to update cost information. Some researcher developed a solution to retrieve data from BIM to reduce the cognitive load of workers (Wang et al., 2014, Chu et al., 2018), they find out that AR can lower workers misinterpretation of drawings and improve their productivity. AR has also been used as a hazard avoidance system to promote health and safety on construction site (Kim et al., 2017a).

Although these studies urge the benefit of BIM and AR, workers still tend to use 2D drawings and checklist to do a job-task. AR applicability and usability in the construction domain is limited due to the functionality of the available tools and its capabilities to transfer information to workers on their exclusive platforms (Wang et al., 2016, Wang et al., 2013, Chu et al., 2018).

2.1 Augmented reality for inspection

Researchers in the BE have shown the potential benefits of AR technology. Inspection is one of the areas that has received attention in recent years. The traditional method of site inspection is a manual based process (e.g., checklist, drawings) where the site manager is in charge of record any deviation between as-built and as designed information. The information needs to be stored in the project database for further action. This process is inefficient, time-consuming and depends on inspector skills and experience to identify the defects (Hernández et al., 2018, Kwon et al., 2014).

A previous study on reinforcing concrete was aimed to improve the manual-based defect system by integrating mobile AR technology, BIM, and image-matching. They proposed a process comprises of two defect system. First, an image-matching system to enable off-site quality inspection. Second, a mobile AR application to give worker or site manager to detect dimension errors and omissions on the job site automatically. An experiment to evaluate the proposed system has proved the effectiveness of the system and can be extended to other applications (Kwon et al., 2014). In tunneling construction (Zhou et al., 2017) investigate the usability of AR technology to detect segment displacement through augmenting quality inspector ability to retrieve QC digital model into the workspace. The main challenge was the accuracy of the tracking approach. The registration of three coordinates, the coordination of inspector AR camera, virtual model coordination and global coordination. A marker-based method has been used in this implementation to overlay the QC digital mode onto the physical environment using mobile AR wearable device. The evaluation experiment has compared the conventional measurement method with the proposed system, which has shown a significant improvement in time over the conventional inspection practice.

Daniel Atherinis et al. (Atherinis et al., 2018) present a system with the purpose of automating falsework inspection. This system utilized radio frequency identification (RFID) and a digital model over a web viewer using mobile devices. The study has concentrated mostly on the efficiency of the RFID component for member identification. The digital model was expected to enable more accurate positional identification of members within the entire falsework configuration. In the laboratory test of RFID technology was faster than the current inspection method, however, for the component positioning test, using the viewer to assess the structure was found to be a more tedious process than checking physical drawings. It was less efficient than the currently practiced method.

Many researchers have found that one of the key challenges of developing an inspection application is the implementation of the appropriate interoperability standards for data exchange in which multiple formats combined in a common standard. The current tools and equipment deployed on-site do not speak the same language (Hernández et al., 2018). Therefore, the intuitive of self-inspection techniques using AR for construction, refurbishment and maintenance of energy-efficient buildings made of prefabricated components (INSITER)(2018) proposed a framework for self-instruction and self-inspection by utilise industry foundation classes (IFC) as a common standard to integrate several technologies such as BIM model viewer, QR reader and generator, dashboard for monitoring and VR/AR features. Under this approach, different data and information can be merged (Hernández et al., 2018). The main goal of INSITER project was to minimize the energy-performance gap between as-designed and as-built.

3. Research Approach

This study is based on an on-site experiment to develop an understanding of the usability of AR technology for QC on the construction site and its potential impact on user performance. Participants in

this study are a diverse group of construction professional from a company based in West Yorkshire, United Kingdom. The experiment was conducted on a construction site of five-storey, 7,500 square meter university building in Huddersfield. This project is BIM-based where all design packages are combined, architecture, structure, and MEP to check for clashes and issues that could affect the construction programme and costs. Participants in this study selected based on their availability in the allocated day. In addition to studying the feasibility of AR application through observing participants' behavior, participants were asked to provide feedback on their overall experience. The following section discusses in detail each step of the research approach.

3.1 Selection of case study

The objective of this study is to improve QC inspection on construction site. The case study was selected based on the current stage of construction progress during the time of the experiment. Thus, the decision was made to check the as-built MEP work and compare it with the as-designed. Since the building is under construction, the chosen spaces for the experiment were restrained to accessibility and health and safety issue. The experiment was carried out in two spaces. The first space is the High Voltage (HV) switch Room 37 m^2, the room was empty, all surfaces are in finish levels such as wall and ceiling, and switchgear was not installed yet see Figure 27. The second space is 261 m^2 open studio, the HVAC system was already installed, finishing work such as drywall and flooring was on progress see *Figure 28*.
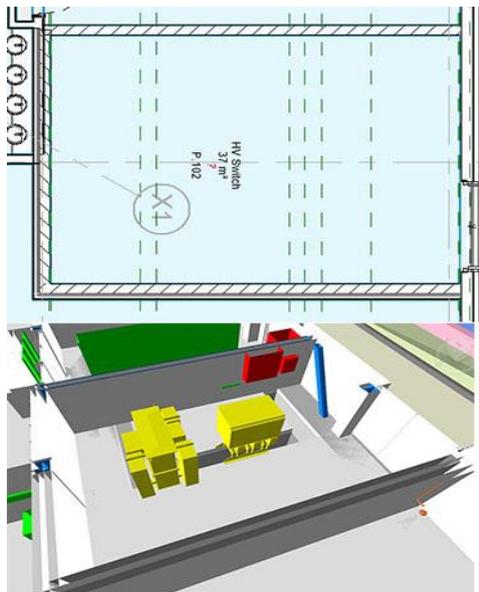
Figure 27: The HV switch Room

Figure 28: The open studio

3.2 Development of BIM AR application

In order to study the impact of AR in the QC inspection process, the development of BIM and AR system is established. A number of different AR devices could have been used theoretically in this experiment such as Daqri and Meta 2. However, the researchers selected Microsoft HoloLens. The HoloLens is a standalone head-mounted display (HMD) with a capability of presenting digital contents over a see-through screen into a physical environment. This headset provides a hands-free operation without the need of physical connection to a computer, which is extremely important to the nature of construction site and the experiment, as it gives the participant a freely move in the space.

To develop BIM and AR solution to examine the MEP system on construction site, all related work packages (e.g., architectural, mechanical, electrical) need to be integrated into one unified BIM platform like Autodesk Navisworks before being exported to Unity game engine. Despite the variety of

methods presented in the previous study (Al-Adhami et al., 2018), forge toolkit has been used in the development of this application. This approach can eliminate the complexity of previous interoperability issues. None of the BIM contents was changed during this process, see *Figure 29* workflow of the development.

Once the BIM model imported to unity, build settings were set to be applicable with HoloLens. Then the scale of the model was verified in the lab to make sure it works at 1:1 scale. The tracing approach of AR application is one of the key challenges. Previous studies claimed that a market-based approach could provide high quality and accurate tracking (Wang et al., 2013, Wang et al., 2014, Zhou et al., 2017). Accordingly, this approach has been adopted after it has proved its effectiveness in the early testing of the application. One of the characteristic features of most AR devices is interacting using a hand gesture, this approach of human-machine interaction (HMI) requires from users to familiarize themselves with the system. Thus, voice commands were included in the application to streamline control of BIM packages for non-expert users.
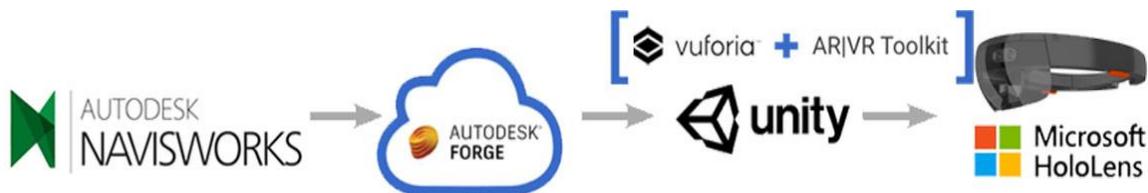
Figure 29: BIM AR Application workflow

3.3 On-site Implementation

The implementation of the system on site comprises three steps. 1) The tracking system of the developed AR application is marker-based, so it requires to set a physical marker on job site to match exactly the one in the digital version; 2) run the application and read the marker using the camera on the HMD (Hololens), this step can determine the coordination of the user in the virtual environment. Therefore, it is essential to set the marker in the first step correctly; 3) once the Hololens recognize the marker, the application began to retrieve BIM data on the job site at 1:1 scale and overlaying the existing structure. Starting from here, the QC inspector can audit the construction work and compare it with the designed model without the need for switching from a physical environment to drawings and vice versa. BIM components and its properties are already stored in the system, the user can pick any component available in the displayed scene using gaze and tap with finger down to retrieve the component properties see *Figure 30*. It is worth to mention that due to construction health and safety (H&S) regulations a Hololens hard hat was used. Although the Hololens hard hat is part of Personal Protective Equipment (PPE), it also distributes the weight of the device and provides a comfortable experience.
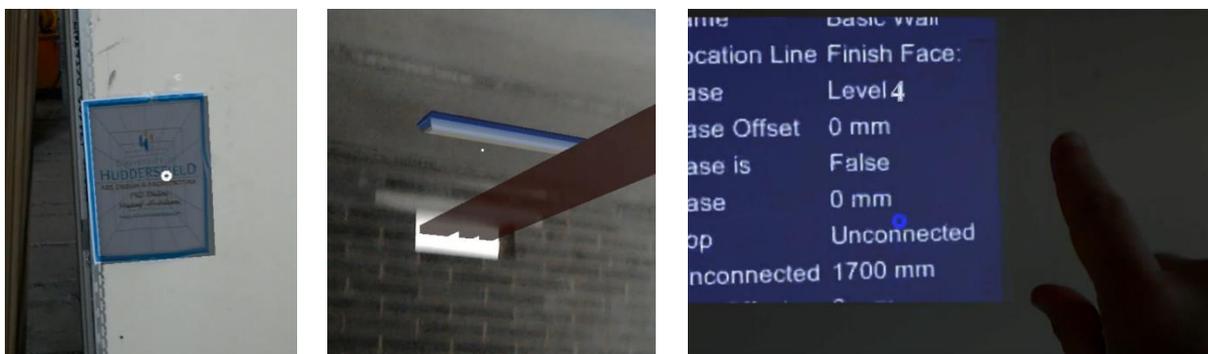
Figure 30: AR implementation

The aim of this study to validate the feasibility of the proposed AR application on the hand of

construction professionals. This is to ensure whether the visualization capability of the current AR devices are mature and can be considered in today's construction framework.

4. Results and discussion

This work demonstrate the utilization of AR application on a job site as part of QC inspection. The results from onsite experiment evaluated based on participants satisfaction, job environment and practicality issues. In this study nine construction professionals participated including BIM manager, design manager, architects, and MEP technicians. In general, they had little or no experience with the AR applications or AR headset. Participants were asked to use the Hololens and run the BIM AR application in the selected spaces, HV switch Room and open studio, to retrieve the MEP model on-site. All participants were able to achieve the task, the AR experience was straightforward and the alignment of the virtual model in the physical space was accurate. However, conducting this experiment on a construction site faced several challenges.

The virtual overlapping on-site is an essential factor of this type of AR applications, it requires to bring BIM geometrical data in real-world scale and fit precisely over the existing structure. This experiment used image-marker technique to achieve this virtual overlapping. The marker needs to be placed in a suitable location in both real and virtual environment that shared the same coordinate. In the HV switch room, the physical image-marker was placed on a finish surface level; this has delivered a precise alignment of holographic data on the job site. While in the second space "open studio," it was hard to find a base point to incorporate both environments "virtual and physical" on the existing structure, as all surfaces were not on finish level and the installed partitions were not reliable. Some participants faced difficulty reading the physical marker, especially in HV switch room as the lighting condition was poor during the time of the experiment and that affected the ability of the hololens to recognize the image-marker. Moreover, the nature of the construction site requires different personnel and activities to interfere which might damage the marker or need to be relocated and that can add more time to the inspection process. Consequently, the marker-based tracking approach is not a practical solution for this type of application.

The narrow field of view (FOV) of the AR headset was one of the main challenges that had an impact on participants' satisfaction. This issue has been recorded during the experiment as participants felt uncomfortable visualizing the model in the HV switch room as they needed to move around to get a clear view. Whereas, in the open studio, participants did not complain of this issue as the task was visualizing the HVAC system in the ceiling which is around 4 meters in height. The HMI using hand gesture was frustrating at the beginning of the experiment as the participants were not familiar with this type of interaction. It has been noticed some of the participants started to switch hands after spending a few minutes of gazing and taping. The added voice command function was useful as it gave easy access to design information, hide/show building elements or retrieve specific data, yet, in high noise spaces, the response was significantly weak.

4.1 Limitations

The experiment has several limitations that can be described as follows: First, none of the participants was from the QC team, and they have no experience in the QC process. As a result, the evaluation can be considered as on hand user experience. Second, despite the experiment took place on a job site, the work environment had been set, cleaned and prepared by the construction company before the experiment started for H&S concerned. Theoretically, the impact would be different as more laborers will be on-site. Furthermore, augmented virtual objects might disconnect the user from reality which can cause H&S issue. Third, the currently available AR devices are suffering from many technical limitations that affect the overall AR experience such as HMI, FOV, HMD weight, and battery life. Moreover, its processing capacity is not adequate to handle heavy geometrical data, this adds more effort and time to the application development process to deliver an acceptable BIM-based AR experience. Thus, it's not practical for everyday on-site activity.
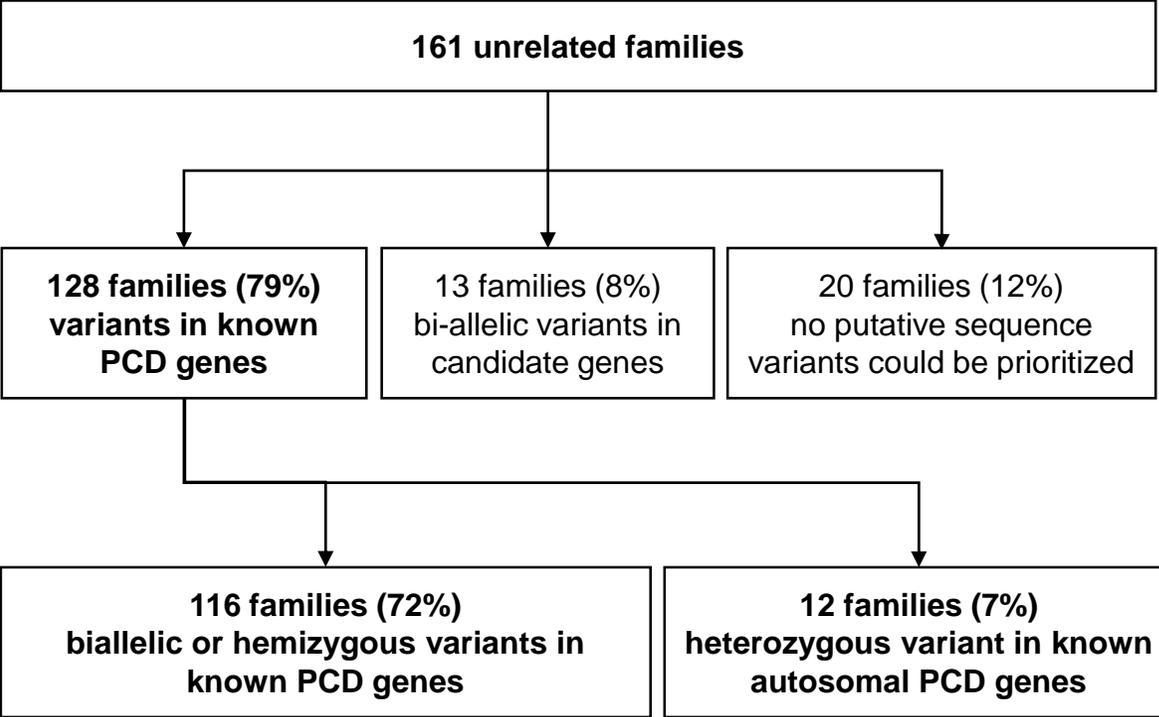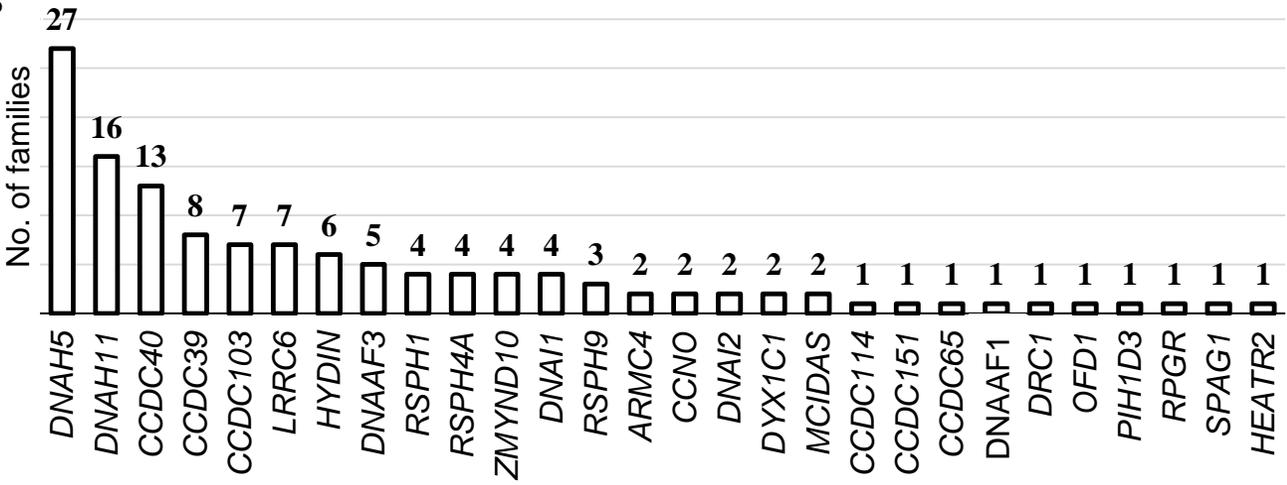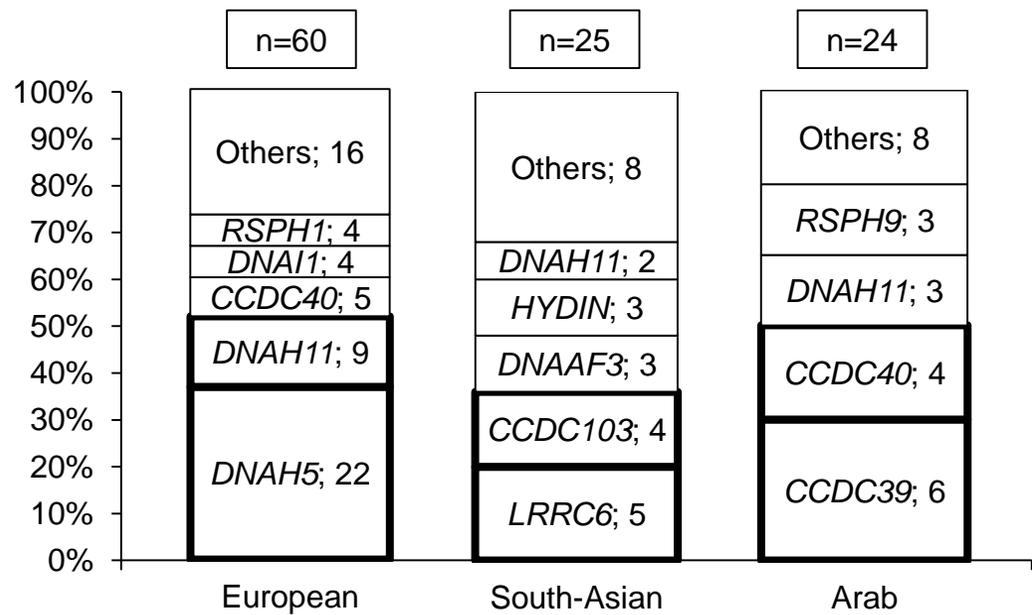
5. Conclusion

Using a checklist and drawings in the inspection process requires switchover between physical and mental process. Hence, the inspector might make some mistakes or omit some content.(Zaeh and Wiesbeck, 2008, Zaeh et al., 2009, Towne, 1985). In this study, an AR system was developed to provide QC inspector an easy access to as-design information, geometrical and textual, on construction site. The developed system used to audit and check the installed MEP works on-site and compare it with the design specification. The application has worked as on-site physical-virtual clash detection based on human observation as this is not an automated process. The developed system has the following features, 1) user can interact with BIM in immersive interactive virtual environment on construction site, 2) virtual overplaying 1:1 scale using image-marker technique, 3) HMI using hand gesture and voice command.
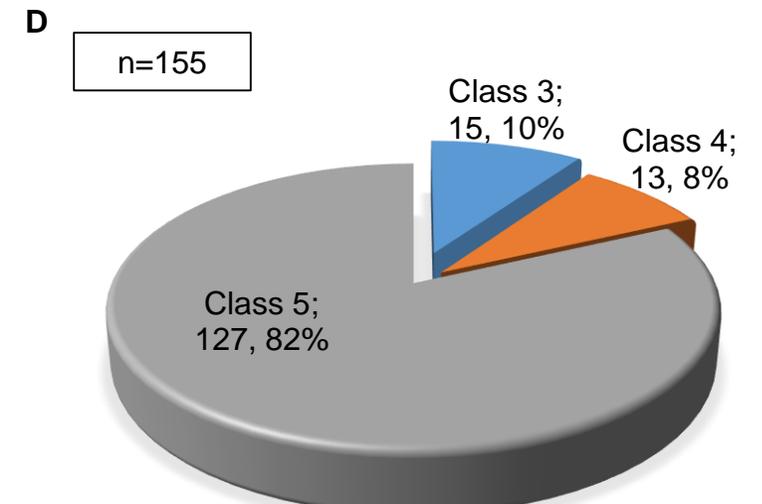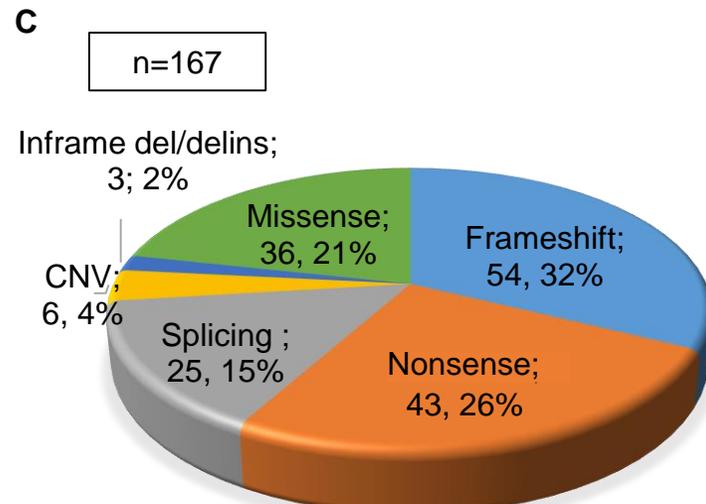
Several limitations and barriers have been explained in accordance with the available AR technology, construction environment, and user perception. The validation method of this study was based on an on-site experiment where construction professionals take part. The developed AR system was used to visualize the HVAC system and switchgear of five-story under construction building. During the analysis on the construction site, the potential benefit of AR has proven, the feedback from the participants have also supported this argument. However, industry professionals have proposed to use it in the office environment for design review or public engagement. Finally, they concluded that the technology not mature, it has several technical limitations and very expensive for daily use on the construction site but they recommended keeping an eye on it latest development as it can bring a great benefit to the construction industry. Although the challenges of the development of the system were not the main concern of this study, future work would be directed toward facing those challenges and quantify the evaluation method.

6. References

2018. *INSITER Project* [Online]. Available: https://www.insiter-project.eu/en [Accessed 23-06-2018 2018].

AGARWALA, C. 2014. Technology and knowledge worker productivity. *Technology,* 102.

AL-ADHAMI, M., MA, L. & WU, S. Exploring Virtual Reality in Construction, Visualization and Building Performance Analysis. 34th International Symposium on Automation and Robotics in Construction, 2018. 969-976.

ARAL, S., BRYNJOLFSSON, E. & VAN ALSTYNE, M. 2012. Information, technology, and information worker productivity. *Information Systems Research,* 23**,** 849-867.

ATHERINIS, D., BAKOWSKI, B., VELCEK, M. & MOON, S. 2018. Developing and Laboratory Testing a Smart System for Automated Falsework Inspection in Construction. *Journal of Construction Engineering and Management,* 144.

BEKELE, M. K., PIERDICCA, R., FRONTONI, E., MALINVERNI, E. S. & GAIN, J. 2018. A survey of augmented, virtual, and mixed reality for cultural heritage. *Journal on Computing and Cultural Heritage,* 11.

BOSCHÉ, F., ABDEL-WAHAB, M. & CAROZZA, L. 2016. Towards a Mixed Reality System for Construction Trade Training. *Journal of Computing in Civil Engineering,* 30.

CHU, M., MATTHEWS, J. & LOVE, P. E. D. 2018. Integrating mobile Building Information Modelling and Augmented Reality systems: An experimental study. *Automation in Construction,* 85**,** 305-316.

DELANEY, B. 2014. *Sex, drugs and tessellation: The truth about virtual reality, as revealed in the pages of CyberEdge Journal*, CyberEdge Information Services.

DRETTAKIS, G., ROUSSOU, M., RECHE, A. & TSINGOS, N. 2007. Design and evaluation of a real-world virtual environment for architecture and urban planning. *Presence: Teleoperators and Virtual Environments,* 16**,** 318-332.

FREINA, L. & OTT, M. A literature review on immersive virtual reality in education: state of the art and perspectives. The International Scientific Conference eLearning and Software for Education, 2015. " Carol I" National Defence University, 133.

HERNÁNDEZ, J. L., LERONES, P. M., BONSMA, P., VAN DELFT, A., DEIGHTON, R. & BRAUN, J. D. 2018. An IFC interoperability framework for self-inspection process in buildings. *Buildings,* 8.

HUANG, T. K., YANG, C. H., HSIEH, Y. H., WANG, J. C. & HUNG, C. C. 2018. Augmented reality (AR) and virtual reality (VR) applied in dentistry. *Kaohsiung Journal of Medical Sciences,* 34**,** 243-248.

JENNIFER WHYTE, D. N. 2018. *Virtual Reality and the Built Environment* Routledge.

KIM, K., KIM, H. & KIM, H. 2017a. Image-based construction hazard avoidance system using augmented reality in wearable device. *Automation in Construction,* 83**,** 390-403.

KIM, Y., KIM, H. & KIM, Y. O. 2017b. Virtual reality and augmented reality in plastic surgery: A review. *Archives of Plastic Surgery,* 44**,** 179-187.

KWON, O. S., PARK, C. S. & LIM, C. R. 2014. A defect management system for reinforced concrete work utilizing BIM, image-matching and augmented reality. *Automation in Construction,* 46**,** 74-81.

LI, X., YI, W., CHI, H. L., WANG, X. & CHAN, A. P. C. 2018. A critical review of virtual and augmented reality (VR/AR) applications in construction safety. *Automation in Construction,* 86**,** 150-162.

LINOWES, J. 2015. *Unity virtual reality projects*, Packt Publishing Ltd.

MAFTEI, L. & HARTY, C. 2015. Designing in caves: Using immersive visualisations in design practice. *Archnet-IJAR,* 9**,** 53-75.

MEŽA, S., TURK, Ž. & DOLENC, M. 2014. Component based engineering of a mobile BIM-based augmented reality system. *Automation in Construction,* 42**,** 1-12.

PAGE, R. L. 2000. Brief history of flight simulation. *SimTecT 2000 Proceedings***,** 11-17.

STEINICKE, F. 2016. *Being Really Virtual*.

TOWNE, D. M. 1985. Cognitive Workload in Fault Diagnosis. UNIVERSITY OF SOUTHERN CALIFORNIA LOS ANGELES BEHAVIORAL TECHNOLOGY LABS.

WANG, X., KIM, M. J., LOVE, P. E. D. & KANG, S.-C. 2013. Augmented Reality in built environment: Classification and implications for future research. *Automation in Construction,* 32**,** 1-13.

WANG, X., ONG, S. K. & NEE, A. Y. 2016. A comprehensive survey of augmented reality assembly research. *Advances in Manufacturing,* 4**,** 1-22.

WANG, X., TRUIJENS, M., HOU, L., WANG, Y. & ZHOU, Y. 2014. Integrating Augmented Reality with Building Information Modeling: Onsite construction process controlling for liquefied natural gas industry. *Automation in Construction,* 40**,** 96-105.

ZAEH, M., WIESBECK, M., STORK, S. & SCHUBOE, A. Factors for a task-induced complexity measure for manual assembly operations. Proc. 3rd Int. Conf. Changeable, Agile, Reconfigurable and Virtual Production (CARV 2009), 2009. München, Germany, 831-845.

ZAEH, M. F. & WIESBECK, M. 2008. A model for adaptively generating assembly instructions using state-based graphs. *Manufacturing systems and technologies for the new frontier.* Springer.

ZAHER, M., GREENWOOD, D. & MARZOUK, M. 2018. Mobile augmented reality applications for construction projects. *Construction Innovation,* 18**,** 152-166.

ZHAO, X. 2017. A scientometric review of global BIM research: Analysis and visualization. *Automation in Construction,* 80**,** 37-47.

ZHOU, Y., LUO, H. & YANG, Y. 2017. Implementation of augmented reality for segment displacement inspection during tunneling construction. *Automation in Construction,* 82**,** 112-121.

A — 161 unrelated families

- 128 families (79%) variants in known PCD genes
- 13 families (8%) bi-allelic variants in candidate genes
- 20 families (12%) no putative sequence variants could be prioritized

- 116 families (72%) biallelic or hemizygous variants in known PCD genes
- 12 families (7%) heterozygous variant in known autosomal PCD genes

B — No. of families

DNAH5: 27, DNAH11: 16, CCDC40: 13, CCDC39: 8, CCDC103: 7, LRRC6: 7, HYDIN: 6, DNAAF3: 5, RSPH1: 4, RSPH4A: 4, ZMYND10: 4, DNAI1: 4, RSPH9: 3, ARMC4: 2, CCNO: 2, DNAI2: 2, DYX1C1: 2, MCIDAS: 2, CCDC114: 1, CCDC151: 1, CCDC65: 1, DNAAF1: 1, DRC1: 1, OFD1: 1, PIH1D3: 1, RPGR: 1, SPAG1: 1, HEATR2: 1

C

European (n=60): DNAH5; 22, DNAH11; 9, CCDC40; 5, DNAI1; 4, RSPH1; 4, Others; 16

South-Asian (n=25): LRRC6; 5, CCDC103; 4, DNAAF3; 3, HYDIN; 3, DNAH11; 2, Others; 8

Arab (n=24): CCDC39; 6, CCDC40; 4, DNAH11; 3, RSPH9; 3, Others; 8

A

Reported before / Not reported before

Top row (cDNA variants): c.232C>T, c.1351C>T, c.1730G>C, c.2710G>T, c.2964_2965del, c.3733C>T, c.5157C>T, c.5177T>C, c.5281C>T, c.5557A>T, c.5710-2A>G, c.5890_5894dup, c.6249G>A, c.6261T>G, c.6763C>T, c.6782T>G, c.6791G>A, c.6930_6934delinsG, c.8320T>C, c.8404C>T, c.8642C>G, c.9480T>A, c.10229C>T, c.10384C>T, c.10601T>C, c.10615C>T, c.10815delT, c.10815T>G, c.11258del, c.11455+5G>A, c.13175T>G, c.13285C>T, c.13458_13459insT, c.13486C>T

DNAH5

Domains: DHC_N1, DHC_N2, AAA+ ATPase, MTB, Dynein_heavy

Bottom row (protein variants): p.Arg78*, p.Gln451*, p.Arg577Thr, p.Glu904*, p.Thr990Asnfs*2, p.Arg1245Cys, p.?, p.Leu1726Pro, p.Arg1761*, p.Lys1853*, p.Cys1904-Lys1909del, p.Leu1966Serfs*9, p.Met2083Ile, p.Tyr2087*, p.Arg2255*, p.Leu2261Arg, p.Ser2264Asn, p.Asn2310Lysfs*15, p.Trp2774Arg, p.Gln2802*, p.Ala2881Gly, p.Cys3160*, p.Thr3410Met, p.Gln3462*, p.Phe3534Ser, p.Arg3539Cys, p.Pro3606Hisfs*22, p.Asp3605Glu, p.Asn3753Thrfs*5, p.?, p.Phe4392Cys, p.Arg4429*, p.Asn4487fs*1, p.Arg4496*

Mutation types: Nonsense, Frameshift, Splicing, Missense

B — n=128

- Homozygous; 74, 58%
- Compound Heterozygous; 39, 31%
- Hemizygous; 3, 2%
- One mutant allele; 12, 9%

C — n=167

- Frameshift; 54, 32%
- Nonsense; 43, 26%
- Splicing; 25, 15%
- CNV; 6, 4%
- Missense; 36, 21%
- Inframe del/delins; 3; 2%

D — n=155

- Class 5; 127, 82%
- Class 4; 13, 8%
- Class 3; 15, 10%

A

DNAI2(p.Arg295*+p.Arg295*)	
DNAI1(p.Ser17Valfs*12+Unknown)	
DNAI1(p.Ser17Valfs*12+p.Ser17Valfs*12)	
DNAH5(p.Arg1761*+p.Thr3410Met)	
DNAH5(p.Pro3606Hisfs*22+Unknown)	
DNAH5(p.Pro3606Hisfs*22 +p.Pro3606Hisfs*22)	
DNAH5(p.Leu1726Pro+p.Arg577Thr)	
DNAH5(p.Arg2255*+p.Cys3160*)	
DNAH5(p.Arg4429*+p.Ala2881Gly)	
DNAH5(p.Leu1966Serfs*9+p.Ser2264Asn)	
DNAH5(p.Asn4487fs*1+p.Phe3534Ser)	
DNAH5(p.Pro3606Hisfs*22 +p.Asn4487fs*1)	
DNAH5(p.Tyr2087*+c.11455+5G>A)	
DNAH5(p.Arg4496*+p.Asn4487fs*1)	

0%   50%   100%

□Both arms present ■IDA Loss only ■ODA Loss only ■Both arms missing

B

LRRC6(p.Trp210Cysfs*12+p.Trp210Cysfs*12)	
LRRC6(p.Trp210Cysfs*12+p.Trp210Cysfs*12)	
LRRC6(p.Trp210Cysfs*12+p.Trp210Cysfs*12)	
LRRC6(p.Trp210Cysfs*12+p.Trp210Cysfs*12)	
HEATR2(p.Arg350Trp+Unknown)	
DYX1C1(Homozygous deletion of exon7)	
DNAAF3(p.Pro344Glyfs*64+p.Gly425*)	
DNAAF3(c.228+5G>C+c.228+5G>C)	
DNAAF3(p.Val208Cysfs*12+p.Val208Cysfs*12)	
DNAAF3(p.Val55Glyfs*28+p.Val55Glyfs*28)	
DNAAF3(p.Glu99Glyfs*88+p.Ala204delinsGlyThr)	
DNAAF1(Homozygous deletion of exon 1,2&3)	

0%   50%   100%

□Both arms present ■IDA Loss only ■ODA Loss only ■Both arms missing